CONCLUSIONS

A SERIES OF studies on response to HCV treatment revealed one of clinical significance on IL-28B. The discovered SNP related to PEG-IFN plus RBV therapy provided the opportunity to investigate the difference between IFNs-λ although these three genes were considered to have a similar function. Considering the function of the IL-28B gene, our findings would suggest that IL-28B behaves as a potentiator of ISG under PEG-IFN plus RBV combination therapy and/or inhibits viral replication by itself. On the other hand, these SNP are useful for the prediction of treatment response because of high OR. This is a first step in the tailor-made therapy for HCV infection. Further studies on IFN-λ and the SNP should be investigated including viral factors such as the mutations in the core and NS5A regions as well as HCVRNA levels to improve positive predictive value for applying practical tailor-made therapy.

REFERENCES

1 Ray Kim W. Global epidemiology and burden of hepatitis C. *Microbes Infect* 2002; **4**: 1219–25.
2 Manns MP, McHutchison JG, Gordon SC *et al.* Peginterferon alfa-2b plus ribavirin compared with interferon alfa-2b plus ribavirin for initial treatment of chronic hepatitis C: a randomised trial. *Lancet* 2001; **358**: 958–65.
3 Fried MW, Shiffman ML, Reddy KR *et al.* Peginterferon alfa-2a plus ribavirin for chronic hepatitis C virus infection. *N Engl J Med* 2002; **347**: 975–82.
4 Hadziyannis SJ, Sette H Jr, Morgan TR *et al.* Peginterferon-alpha2a and ribavirin combination therapy in chronic hepatitis C: a randomized study of treatment duration and ribavirin dose. *Ann Intern Med* 2004; **140**: 346–55.
5 Fried MW. Side effects of therapy of hepatitis C and their management. *Hepatology* 2002; **36**: S237–44.
6 Pascu M, Martus P, Hohne M *et al.* Sustained virological response in hepatitis C virus type 1b infected patients is predicted by the number of mutations within the NS5A-ISDR: a meta-analysis focused on geographical differences. *Gut* 2004; **53**: 1345–51.
7 Shirakawa H, Matsumoto A, Joshita S *et al.* Pretreatment prediction of virological response to peginterferon plus ribavirin therapy in chronic hepatitis C patients using viral and host factors. *Hepatology* 2008; **48**: 1753–60.
8 Akuta N, Suzuki F, Sezaki H *et al.* Association of amino acid substitution pattern in core protein of hepatitis C virus genotype 1b high viral load and non-virological response to interferon-ribavirin combination therapy. *Intervirology* 2005; **48**: 372–80.
9 Walsh MJ, Jonsson JR, Richardson MM *et al.* Non-response to antiviral therapy is associated with obesity and increased hepatic expression of suppressor of cytokine signalling 3 (SOCS-3) in patients with chronic hepatitis C, viral genotype 1. *Gut* 2006; **55**: 529–35.
10 Gao B, Hong F, Radaeva S. Host factors and failure of interferon-alpha treatment in hepatitis C virus. *Hepatology* 2004; **39**: 880–90.
11 Matsuyama N, Mishiro S, Sugimoto M *et al.* The dinucleotide microsatellite polymorphism of the IFNAR1 gene promoter correlates with responsiveness of hepatitis C patients to interferon. *Hepatol Res* 2003; **25**: 221–5.
12 Tsukada H, Ochi H, Maekawa T *et al.* A polymorphism in MAPKAPK3 affects response to interferon therapy for chronic hepatitis C. *Gastroenterology* 2009.
13 Suppiah V, Moldovan M, Ahlenstiel G *et al.* IL28B is associated with response to chronic hepatitis C interferon-alpha and ribavirin therapy. *Nat Genet* 2009; **41**: 1100–4.
14 Ank N, Iversen MB, Bartholdy C *et al.* An important role for type III interferon (IFN-lambda/IL-28) in TLR-induced antiviral activity. *J Immunol* 2008; **180**: 2474–85.
15 Ge D, Fellay J, Thompson AJ *et al.* Genetic variation in IL28B predicts hepatitis C treatment-induced viral clearance. *Nature* 2009; **461**: 399–401.
16 Tanaka Y, Nishida N, Sugiyama M *et al.* Genome-wide association of IL28B with response to pegylated interferon-alpha and ribavirin therapy for chronic hepatitis C. *Nat Genet* 2009; **41**: 1105–9.
17 Thomas DL, Thio CL, Martin MP *et al.* Genetic variation in IL28B and spontaneous clearance of hepatitis C virus. *Nature* 2009; **461**: 798–801.
18 Gad HH, Dellgren C, Hamming OJ, Vends S, Paludan SR, Hartmann R. Interferon-lambda is functionally an interferon but structurally related to the interleukin-10 family. *J Biol Chem* 2009; **284**: 20869–75.
19 Sheppard P, Kindsvogel W, Xu W *et al.* IL-28, IL-29 and their class II cytokine receptor IL-28R. *Nat Immunol* 2003; **4**: 63–8.
20 Siren J, Pirhonen J, Julkunen I, Matikainen S. IFN-alpha regulates TLR-dependent gene expression of IFN-alpha, IFN-beta, IL-28, and IL-29. *J Immunol* 2005; **174**: 1932–7.
21 Onoguchi K, Yoneyama M, Takemura A *et al.* Viral infections activate types I and III interferon genes through a common mechanism. *J Biol Chem* 2007; **282**: 7576–81.
22 Osterlund PI, Pietila TE, Veckman V, Kotenko SV, Julkunen I. IFN regulatory factor family members differentially regulate the expression of type III IFN (IFN-lambda) genes. *J Immunol* 2007; **179**: 3434–42.
23 Sommereyns C, Paul S, Staeheli P, Michiels T. IFN-lambda (IFN-lambda) is expressed in a tissue-dependent fashion and primarily acts on epithelial cells in vivo. *Plos Pathog* 2008; **4**: e1000017.
24 Zhou L, Wang X, Wang YJ *et al.* Activation of toll-like receptor-3 induces interferon-lambda expression in human neuronal cells. *Neuroscience* 2009; **159**: 629–37.

25 Jaitin DA, Roisman LC, Jaks E *et al.* Inquiring into the differential action of interferons (IFNs): an IFN-alpha2 mutant with enhanced affinity to IFNAR1 is functionally similar to IFN-beta. *Mol Cell Biol* 2006; 26: 1888–97.

26 Jaks E, Gavutis M, Uze G, Martal J, Piehler J. Differential receptor subunit affinities of type 1 interferons govern differential signal activation. *J Mol Biol* 2007; 366: 525–39.

27 Kotenko SV, Gallagher G, Baurin VV *et al.* IFN-lambdas mediate antiviral protection through a distinct class II cytokine receptor complex. *Nat Immunol* 2003; 4: 69–77.

28 Mordstein M, Kochs G, Dumoutier L *et al.* Interferon-lambda contributes to innate immunity of mice against influenza A virus but not against hepatotropic viruses. *Plos Pathog* 2008; 4: e1000151.

29 Witte K, Gruetz G, Volk HD *et al.* Despite IFN-lambda receptor expression, blood immune cells, but not keratinocytes or melanocytes, have an impaired response to type III interferons: implications for therapeutic applications of these cytokines. *Genes Immun* 2009; 10: 702–14.

30 Donnelly RP, Sheikh F, Kotenko SV, Dickensheets H. The expanded family of class II cytokines that share the IL-10 receptor-2 (IL-10R2) chain. *J Leukoc Biol* 2004; 76: 314–21.

31 Hikami K, Ehara Y, Hasegawa M *et al.* Association of IL-10 receptor 2 (IL10RB) SNP with systemic sclerosis. *Biochem Biophys Res Commun* 2008; 373: 403–7.

32 Dumoutier L, Tounsi A, Michiels T, Sommereyns C, Kotenko SV, Renauld JC. Role of the interleukin (IL)-28 receptor tyrosine residues for antiviral and antiproliferative activity of IL-29/interferon-lambda 1: similarities with type I interferon signaling. *J Biol Chem* 2004; 279: 32269–74.

33 Hou W, Wang X, Ye L *et al.* Lambda interferon inhibits human immunodeficiency virus type 1 infection of macrophages. *J Virol* 2009; 83: 3834–42.

34 Serra C, Biolchini A, Mei A, Kotenko S, Dolei A. Type III and I interferons increase HIV uptake and replication in human cells that overexpress CD4, CCR5, and CXCR4. *AIDS Res Hum Retroviruses* 2008; 24: 173–80.

35 Ank N, West H, Bartholdy C, Eriksson K, Thomsen AR, Paludan SR. Lambda interferon (IFN-lambda), a type III IFN, is induced by viruses and IFNs and displays potent antiviral activity against select virus infections in vivo. *J Virol* 2006; 80: 4501–9.

36 Dellgren C, Gad HH, Hamming OJ, Melchjorsen J, Hartmann R. Human interferon-lambda3 is a potent member of the type III interferon family. *Genes Immun* 2009; 10: 125–31.

37 Meager A, Visvalingam K, Dilger P, Bryan D, Wadhwa M. Biological activity of interleukins-28 and -29: comparison with type I interferons. *Cytokine* 2005; 31: 109–18.

38 Stoltz M, Ahlm C. Lundkvist A and Klingstrom J. Lambda interferon (IFN-lambda) in serum is decreased in hantavirus-infected patients, and in vitro-established infection is insensitive to treatment with all IFNs and inhibits IFN-gamma-induced nitric oxide production. *J Virol* 2007; 81: 8685–91.

39 Wang J, Oberley-Deegan R, Wang S *et al.* Differentiated human alveolar type II cells secrete antiviral IL-29 (IFN-lambda 1) in response to influenza A infection. *J Immunol* 2009; 182: 1296–304.

40 Osterlund P, Veckman V, Siren J *et al.* Gene expression and antiviral activity of alpha/beta interferons and interleukin-29 in virus-infected human myeloid dendritic cells. *J Virol* 2005; 79: 9608–17.

41 Hong SH, Cho O, Kim K, Shin HJ, Kotenko SV, Park S. Effect of interferon-lambda on replication of hepatitis B virus in human hepatoma cells. *Virus Res* 2007; 126: 245–9.

42 Doyle SE, Schreckhise H, Khuu-Duong K *et al.* Interleukin-29 uses a type 1 interferon-like program to promote antiviral responses in human hepatocytes. *Hepatology* 2006; 44: 896–906.

43 Robek MD, Boyd BS, Chisari FV. Lambda interferon inhibits hepatitis B and C virus replication. *J Virol* 2005; 79: 3851–4.

44 Marcello T, Grakoui A, Barba-Spaeth G *et al.* Interferons alpha and lambda inhibit hepatitis C virus replication with distinct signal transduction and gene regulation kinetics. *Gastroenterology* 2006; 131: 1887–98.

45 Zhu H, Butera M, Nelson DR, Liu C. Novel type I interferon IL-28A suppresses hepatitis C viral RNA replication. *Virol J* 2005; 2: 80.

46 Brand S, Zitzmann K, Dambacher J *et al.* SOCS-1 inhibits expression of the antiviral proteins 2′,5′-OAS and MxA induced by the novel interferon-lambdas IL-28A and IL-29. *Biochem Biophys Res Commun* 2005; 331: 543–8.

°⊛EASL | JOURNAL OF HEPATOLOGY

Pre-treatment prediction of response to pegylated-interferon plus ribavirin for chronic hepatitis C using genetic polymorphism in *IL28B* and viral factors

Masayuki Kurosaki[1], Yasuhito Tanaka[2], Nao Nishida[3], Naoya Sakamoto[4], Nobuyuki Enomoto[5], Masao Honda[6], Masaya Sugiyama[2], Kentaro Matsuura[2], Fuminaka Sugauchi[2], Yasuhiro Asahina[1], Mina Nakagawa[4], Mamoru Watanabe[4], Minoru Sakamoto[5], Shinya Maekawa[5], Akito Sakai[6], Shuichi Kaneko[6], Kiyoaki Ito[7], Naohiko Masaki[7], Katsushi Tokunaga[3], Namiki Izumi[1,*], Masashi Mizokami[2,7]

[1]Division of Gastroenterology and Hepatology, Musashino Red Cross Hospital, Tokyo, Japan; [2]Department of Virology, Liver Unit, Nagoya City University, Graduate School of Medical Sciences, Nagoya, Japan; [3]Department of Human Genetics, Graduate School of Medicine, University of Tokyo, Tokyo, Japan; [4]Department of Gastroenterology and Hepatology, Tokyo Medical and Dental University, Tokyo, Japan; [5]First Department of Internal Medicine, University of Yamanashi, Yamanashi, Japan; [6]Department of Gastroenterology, Kanazawa University, Graduate School of Medicine, Kanazawa, Japan; [7]Research Center for Hepatitis and Immunology, International Medical Center of Japan, Konodai Hospital, Ichikawa, Japan

Background & Aims: Pegylated interferon and ribavirin (PEG-IFN/RBV) therapy for chronic hepatitis C virus (HCV) genotype 1 infection is effective in 50% of patients. Recent studies revealed an association between the *IL28B* genotype and treatment response. We aimed to develop a model for the pre-treatment prediction of response using host and viral factors.
Methods: Data were collected from 496 patients with HCV genotype 1 treated with PEG-IFN/RBV at five hospitals and universities in Japan. *IL28B* genotype and mutations in the core and IFN sensitivity determining region (ISDR) of HCV were analyzed to predict response to therapy. The decision model was generated by data mining analysis.
Results: The *IL28B* polymorphism correlated with early virological response and predicted null virological response (NVR) (odds ratio = 20.83, p <0.0001) and sustained virological response (SVR) (odds ratio = 7.41, p <0.0001) independent of other covariates. Mutations in the ISDR predicted relapse and SVR independent of *IL28B*. The decision model revealed that patients with the minor *IL28B* allele and low platelet counts had the highest NVR (84%) and lowest SVR (7%), whereas those with the major *IL28B* allele and mutations in the ISDR or high platelet counts had the lowest NVR (0–17%) and highest SVR (61–90%). The model had high reproducibility and predicted SVR with 78% specificity and 70% sensitivity.

Conclusions: The *IL28B* polymorphism and mutations in the ISDR of HCV were significant pre-treatment predictors of response to PEG-IFN/RBV. The decision model, including these host and viral factors may support selection of optimum treatment strategy for individual patients.

Introduction

Hepatitis C virus (HCV) infection is the leading cause of cirrhosis and hepatocellular carcinoma worldwide [1]. The successful eradication of HCV, defined as a sustained virological response (SVR), is associated with a reduced risk of developing hepatocellular carcinoma. Currently, pegylated interferon (PEG-IFN) plus ribavirin (RBV) is the most effective standard of care for chronic hepatitis C but the rate of SVR is around 50% in patients with HCV genotype 1 [2,3], the most common genotype in Japan, Europe, the United States, and many other countries. Moreover, 20–30% of patients with HCV genotype 1 have a null virological response (NVR) to PEG-IFN/RBV therapy [4]. The most reliable method for predicting the response is to monitor the early decline of serum HCV-RNA levels during treatment [5] but there is no established method for prediction before treatment. Because PEG-IFN/RBV therapy is costly and often accompanied by adverse effects such as flu-like symptoms, depression and hematological abnormalities, pre-treatment predictions of those patients who are unlikely to benefit from this regimen enables ineffective treatment to be avoided.

Recently, it has been reported through a genome-wide association study (GWAS) of patients with genotype 1 HCV that single nucleotide polymorphisms (SNPs) located near the *IL28B* gene are strongly associated with a response to PEG-IFN/RBV therapy in

ELSEVIER

Research Article

Table 1. Baseline characteristics of all patients, and patients assigned to the model building or validation groups.

	All patients n = 496	Model group n = 331	Validation group n = 165
Gender: male	250 (50%)	170 (51%)	80 (48%)
Age (years)	57.1 ± 9.9	56.8 ± 9.7	57.5 ± 10.2
ALT (IU/L)	78.6 ± 60.8	78.1 ± 61.4	79.7 ± 59.6
GGT (IU/L)	59.3 ± 63.6	58.9 ± 62.0	60.2 ± 66.9
Platelets (10^9/L)	154 ± 53	153 ± 52	154 ± 56
Fibrosis: F3-4	121 (24%)	80 (24%)	41 (25%)
HCV-RNA: >600,000 IU/ml	409 (82%)	273 (82%)	136 (82%)
ISDR mutation: ≤1	220 (88%)	290 (88%)	145 (88%)
Core 70 (Arg/Gln or His)	293 (59%)/203 (41%)	197 (60%)/134 (40%)	96 (58%)/69 (42%)
Core 91 (Leu/Met)	299 (60%)/197 (40%)	200 (60%)/131 (40%)	99 (60%)/66 (40%)
IL28B: Minor allele	151 (30%)	101 (31%)	50 (30%)
SVR	194 (39%)	129 (39%)	65 (39%)
Relapse	152 (31%)	103 (31%)	49 (30%)
NVR	150 (30%)	99 (30%)	51 (31%)

ALT, alanine aminotransferase; GGT, gamma-glutamyltransferase; ISDR, interferon sensitivity determining region; Arg, arginine; Gln, glutamine; His, histidine; Leu, leucine; Met, methionine; Minor, heterozygote or homozygote of minor allele; SVR, sustained virological response; NVR, null virological response.

Japanese [6], European [7], and a multi-ethnic population [8,9]. The last three studies focused on the association of SNPs in the *IL28B* region with SVR [7–9] but we found a stronger association with NVR [6]. In addition to these host genetic factors, we have reported that mutations within a stretch of 40 amino acids in the NS5A region of HCV, designated as the IFN sensitivity determining region (ISDR), are closely associated with the virological response to IFN therapy: a lower number of mutations is associated with treatment failure [10–13]. Amino acid substitutions at positions 70 and 91 of the HCV core region (Core70, Core91) also have been reported to be associated with response to PEG-IFN/RBV therapy: glutamine (Gln) or histidine (His) at Core70 and methionine (Met) at Core91 are associated with treatment resistance [4,14]. The importance of substitutions in the HCV core and ISDR was confirmed recently by a Japanese multicenter study [15]. How these viral factors contribute to response to therapy is yet to be determined. For general application in clinical practice, host genetic factors and viral factors should be considered together.

Data mining analysis is a family of non-parametric regression methods for predictive modeling. Software is used to automatically explore the data to search for optimal split variables and to build a decision tree structure [16]. The major advantage of decision tree analysis over logistic regression analysis is that the results of the analysis are presented in the form of flow chart, which can be interpreted intuitively and readily made available for use in clinical practice [17]. The decision tree analysis has been utilized to define prognostic factors in various diseases [18–25]. We have reported recently its usefulness for the prediction of an early virological response (undetectable HCV-RNA within 12 weeks of therapy) to PEG-IFN/RBV therapy in chronic hepatitis C [26].

This study aimed to define the pre-treatment prediction of response to PEG-IFN/RBV therapy through the integrated analysis of host factors, such as the *IL28B* genetic polymorphism and various clinical covariates, as well as viral factors, such as mutations in the HCV core and ISDR and serum HCV-RNA load. In addition,

for the general application of these results in clinical practice, decision models for the pre-treatment prediction of response were determined by data mining analysis.

Materials and methods

Patients

This was a multicentre retrospective study supported by the Japanese Ministry of Health, Labor and Welfare. Data were collected from a total of 496 chronic hepatitis C patients who were treated with PEG-IFN alpha and RBV at five hospitals and universities throughout Japan. Of these, 98 patients also were included in the original GWAS analysis [6]. The inclusion criteria in this study were as follows (1) infection by genotype 1b, (2) lack of co-infection with hepatitis B virus or human immunodeficiency virus, (3) lack of other causes of liver disease, such as autoimmune hepatitis, and primary biliary cirrhosis, (4) completion of at least 24 weeks of therapy, (5) adherence of more than 80% to the planned dose of PEG-IFN and RBV for the NVR patients, (6) availability of DNA for the analysis of the genetic polymorphism of *IL28B*, and (7) availability of serum for the determination of mutations in the ISDR and substitutions of Core70 and Core91 of HCV. Patients received PEG-IFN alpha-2a (180 μg) or 2b (1.5 μg/kg) subcutaneously every week and were administered a weight adjusted dose of RBV (600 mg for <60 kg, 800 mg for 60–80 kg, and 1000 mg for >80 kg daily) which is the recommended dosage in Japan. Written informed consent was obtained from each patient and the study protocol conformed to the ethical guidelines of the Declaration of Helsinki and was approved by the institutional ethics review committee. The baseline characteristics are listed in Table 1. For the data mining analysis, 67% of the patients (331 patients) were assigned randomly to the model building group and 33% (165 patients) to the validation group. There were no significant differences in the clinical backgrounds between these two groups.

Laboratory and histological tests

Blood samples were obtained before therapy and were analyzed for hematologic tests and for blood chemistry and HCV-RNA. Sequences of ISDR and the core region of HCV were determined by direct sequencing after amplification by reverse-transcription and polymerase chain reaction as reported previously [4,11]. Genetic polymorphism in one tagging SNP located near the *IL28B* gene (rs8099917) was determined by the GWAS or DigiTag2 assay [27]. Homozygosity (GG) or heterozygosity (TG) of the minor sequence was defined as having the *IL28B* minor allele, whereas homozygosity for the major sequence (TT) was
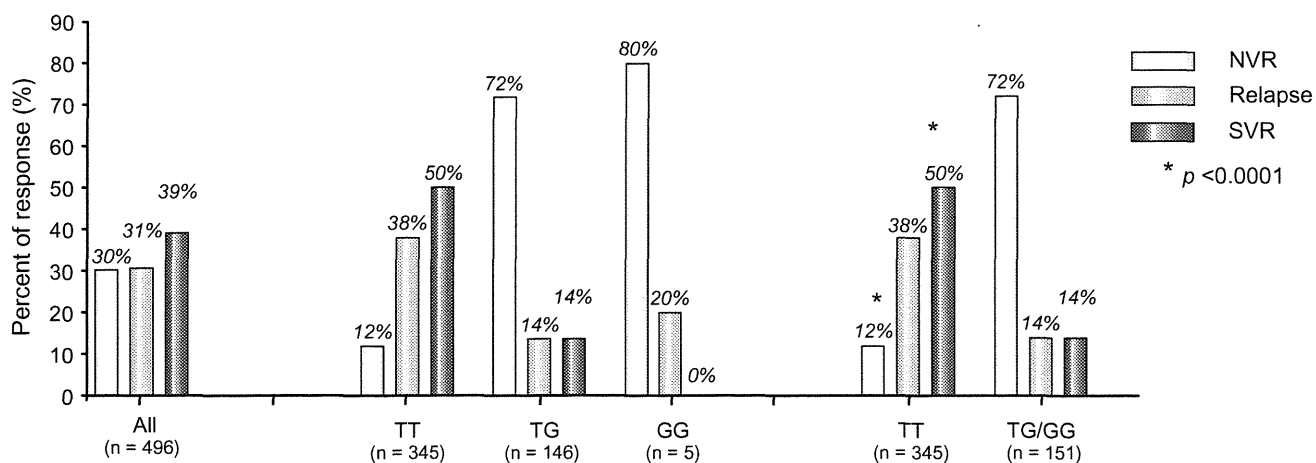
440

Fig. 1. Association between the IL28B genotype (rs8099917) and treatment response. The rates of response to treatment are shown for each rs8099917 genotype. The rate of null virological response (NVR), relapse, and sustained virological response (SVR) is shown. The p values are from Fisher's exact test. The rate of NVR was significantly higher (p <0.0001) and the rate of SVR was significantly lower (p <0.0001) in patients with the IL28B minor allele compared to those with the major allele.

defined as having the IL28B major allele. In this study, NVR was defined as a less than 2 log reduction of HCV-RNA at week 12 and detectable HCV-RNA by qualitative PCR with a lower detection limit of 50 IU/ml (Amplicor, Roche Diagnostic systems, CA) at week 24 during therapy. RVR (rapid virological response) and complete early virological response (cEVR) were defined as undetectable HCV-RNA at 4 weeks and 12 weeks during therapy and SVR was defined as undetectable HCV-RNA 24 weeks after the completion of therapy. Relapse was defined as reappearance of HCV-RNA after the completion of therapy. The stage of liver fibrosis was scored according to the METAVIR scoring system: F0 (no fibrosis), F1 (mild fibrosis: portal fibrosis without septa), F2 (moderate fibrosis: few septa), F3 (severe fibrosis: numerous septa without cirrhosis) and F4 (cirrhosis). Percentage of steatosis was quantified in 111 patients by determining the average proportion of hepatocytes affected by steatosis.

Statistical analysis

Associations between pre-treatment variables and treatment response were analyzed by univariate and multivariate logistic regression analysis. Associations between the IL28B polymorphism and sequences of HCV were analyzed by Fisher's exact test. SPSS software v.15.0 (SPSS Inc., Chicago, IL) was used for these analyses. For the data mining analysis, IBM-SPSS Modeler version 13.0 (IBM-SPSS Inc., Chicago, IL) software was utilized as reported previously [26]. The patients used for model building were divided into two groups at each step of the analysis based on split variables. Each value of each variable was considered as a potential split. The optimum variables and cut-off values were determined by a statistical search algorithm to generate the most significant division into two prognostic subgroups that were as homogeneous as possible for the probability of SVR. Thereafter, each subgroup was evaluated again and divided further into subgroups. This procedure was repeated until no additional significant variable was detected or the sample size was below 15. To avoid over-fitting, 10-fold cross validation was used in the tree building process. The reproducibility of the resulting model was tested with the data from the validation patients.

Results

Association between the IL28B (rs8099917) genotype and the PEG-IFN/RBV response

The rs8099917 allele frequency was 70% for TT (n = 345), 29% for TG (n = 146), and 1% for GG (n = 5). We defined the IL28B major allele as homozygous for the major sequence (TT) and the IL28B minor allele as homozygous (GG) or heterozygous (TG) for the minor sequence. The rate of NVR was significantly higher (72% vs. 12%, p <0.0001) and the rate of SVR was significantly lower (14% vs. 50%, p <0.0001) in patients with the IL28B minor allele compared to those with the major allele (Fig. 1).

Effect of the IL28B polymorphism, substitutions in the ISDR, Core70, and Core91 of HCV on time-dependent clearance of HCV

Patients were stratified according to their IL28B allele type, the number of mutations in the ISDR, the amino acid substitutions in Core70 and Core91, and the rate of undetectable HCV-RNA at 4, 8, 12, 24, and 48 weeks after the start of therapy were analyzed (Fig. 2A–D). The rate of undetectable HCV-RNA was significantly higher in patients with the IL28B major allele than the minor allele, in patients with two or more mutations in the ISDR compared to none or only one mutation, in patients with arginine (Arg) at Core70 rather than Gln/His, and in patients with leucine (Leu) at Core91 rather than Met. The difference was most significant when stratified by the IL28B allele type. The rate of RVR and cEVR was significantly more frequent in patients with the IL28B major allele compared with those with the IL28B minor allele: 9% vs. 3% for RVR (p <0.005) and 57% vs. 11% for cEVR (p <0.0001). These findings suggest that IL28B has the greatest impact on early virological response to therapy.

Association between substitutions in the ISDR and relapse after the completion of therapy

Patients were stratified according to the IL28B allele, number of mutations in the ISDR, and amino acid substitutions of Core70 and Core91, and the rate of relapse was analyzed (Fig. 3A and B). Among patients who achieved cEVR, the rate of relapse was significantly lower in patients with two or more mutations in the ISDR compared to those with only one or no mutations (15% vs. 31%, p <0.005) (Fig. 3 B). On the other hand, the relapse rate was not different between the IL28B major and minor alleles within patients who achieved RVR (3% vs. 0%) or cEVR (28% vs. 29%) (Fig. 3A). Amino acid substitutions of Core70 and Core91 were not associated with the rate of relapse (data not shown).

Factors associated with response by multivariate logistic regression analysis

By univariate analysis, the minor allele of IL28B (p <0.0001), one or no mutations in the ISDR (p = 0.03), high serum level of
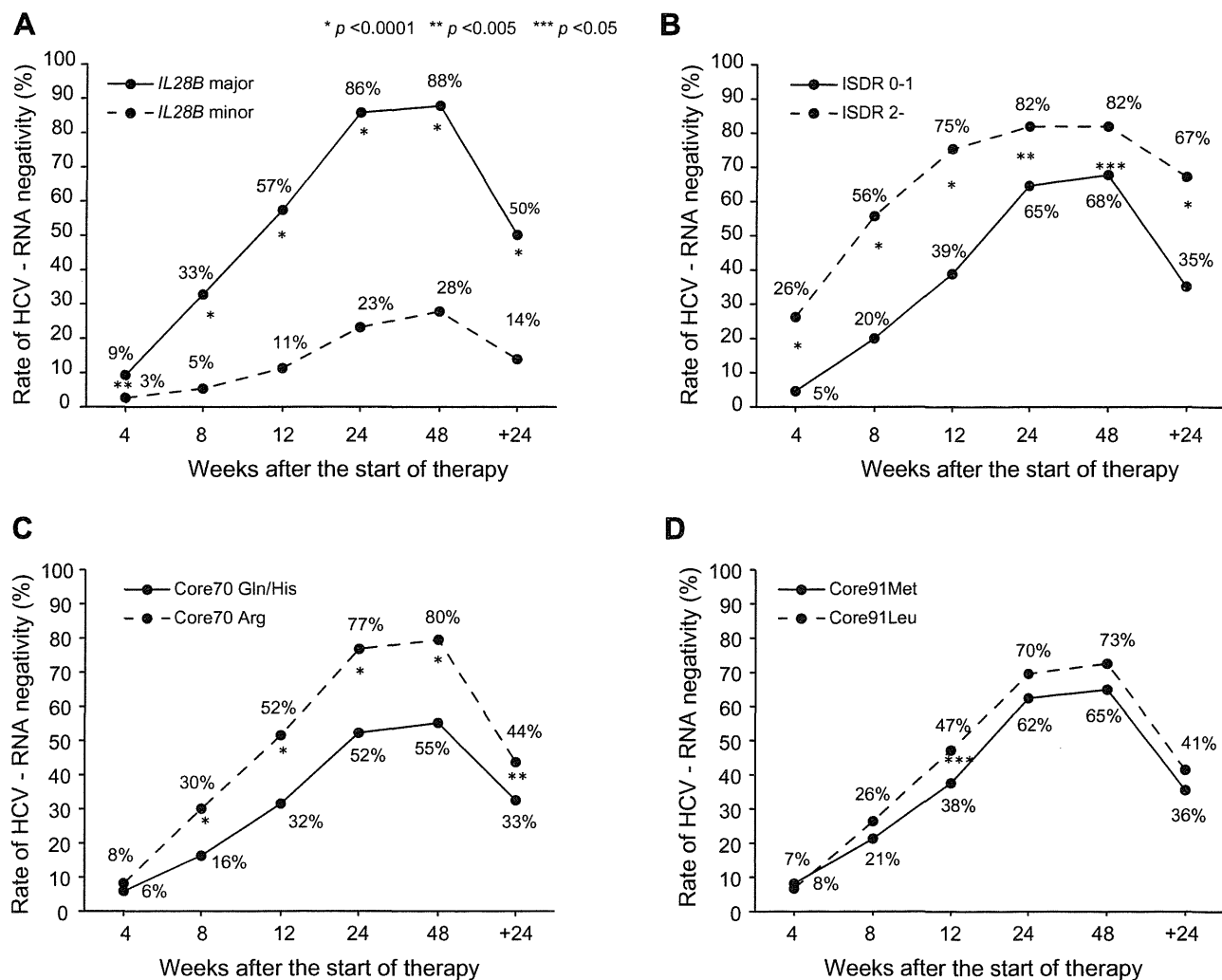
Research Article

A   * p <0.0001   ** p <0.005   *** p <0.05   **B**

Rate of HCV - RNA negativity (%)

IL28B major
IL28B minor

86%   88%
57%
50%
33%
23%   28%
14%
9%   5%   11%
3%

Weeks after the start of therapy
4   8   12   24   48   +24

Rate of HCV - RNA negativity (%)

ISDR 0-1
ISDR 2-

82%   82%
75%   67%
56%   65%   68%
39%   35%
26%
20%
5%

Weeks after the start of therapy
4   8   12   24   48   +24

C   **D**

Rate of HCV - RNA negativity (%)

Core70 Gln/His
Core70 Arg

77%   80%
52%
52%   55%   44%
30%   32%   33%
8%   16%
6%

Weeks after the start of therapy
4   8   12   24   48   +24

Rate of HCV - RNA negativity (%)

Core91Met
Core91Leu

70%   73%
47%   62%   65%
26%   38%   41%
7%   21%   36%
8%

Weeks after the start of therapy
4   8   12   24   48   +24

Fig. 2. **Effect of IL28B mutations in the ISDR, Core70, and Core91 of HCV on time-dependent clearance of HCV.** The rate of undetectable HCV-RNA was plotted for serial time points after the start of therapy (4, 8, 12, 24, and 48 weeks) and for 24 weeks after the completion of therapy. Patients were stratified according to (A) the IL28B allele (minor allele vs. major allele), (B) the number of mutations in the ISDR (0–1 mutation vs. 2 or more mutations), amino acid substitutions of (C) Core70 (Gln/His vs. Arg), and (D) Core91 (Met vs. Leu). The p values are from Fisher's exact test.

HCV-RNA ($p = 0.035$), Gln or His at Core70 ($p < 0.0001$), low platelet counts ($p = 0.009$), and advanced fibrosis ($p = 0.0002$) were associated with NVR. By multivariate analysis, the minor allele of IL28B (OR = 20.83, 95%CI = 11.63–37.04, $p < 0.0001$) was associated with NVR independent of other covariates (Table 2). Notably, mutations in the ISDR ($p = 0.707$) and at amino acid Core70 ($p = 0.207$) were not significant in multivariate analysis due to the positive correlation with the IL28B polymorphism ($p = 0.004$ for ISDR and $p < 0.0001$ for Core70, Fig. 4).

Genetic polymorphism of IL28B also was associated with SVR (OR = 7.41, 95% CI = 4.05–13.57, $p < 0.0001$) independent of other covariates, such as platelet counts, fibrosis, and serum levels of HCV-RNA. Mutation in the ISDR was an independent predictor of SVR (OR = 2.11, 95% CI = 1.06–4.18, $p = 0.033$) but the amino acid at Core70 was not (Table 3).

Factors associated with the IL28B polymorphism

Patients with the IL28B minor allele had significantly higher serum level of gamma-glutamyltransferase (GGT) and a higher

frequency of hepatic steatosis (Table 4). When the association between the IL28B polymorphism and HCV sequences was analyzed, Gln or His at Core70, that is linked to resistance to PEG-IFN and RBV therapy [4,14,15], was significantly more frequent in patients with the minor IL28B allele than in those with the major allele (67% vs. 30%, $p < 0.0001$) (Fig. 4). Other HCV sequences with an IFN resistant phenotype also were more prevalent in patients with the minor IL28B allele than those with the major allele: Met at Core91 (46% vs. 37%, $p = 0.047$) and one or no mutations in the ISDR (94% vs. 85%, $p = 0.004$) (Fig. 4).

Data mining analysis

Data mining analysis was performed to build a model for the prediction of SVR and the result is shown in Fig. 5. The analysis selected four predictive variables, resulting in six subgroups of patients. Genetic polymorphism of IL28B was selected as the best predictor of SVR. Patients with the minor IL28B allele had a lower probability of SVR and a higher probability of NVR than those with the major IL28B allele (SVR: 14% vs. 50%, NVR: 72% vs.
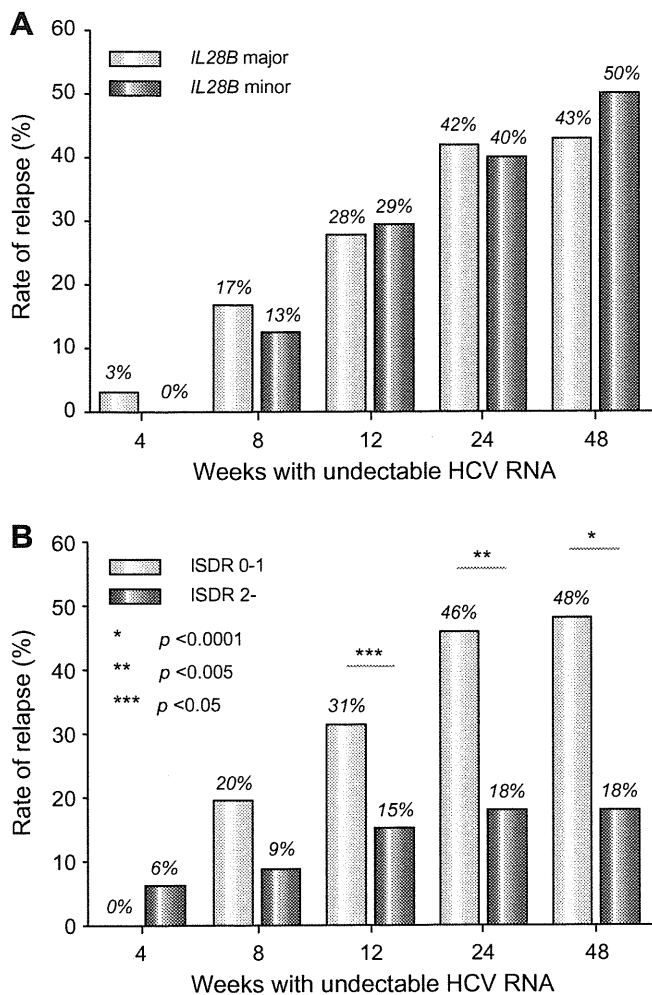
97
122

A

B

Fig. 3. **Association between relapse and the** *IL28B* **allele or mutations in the ISDR.** The rate of relapse was calculated for patients who had undetectable HCV-RNA at serial time points after the start of therapy (4, 8, 12, 24, and 48 weeks). Patients were stratified according to (A) the *IL28B* allele (minor allele vs. major allele) and (B) the number of mutations in the ISDR (0–1 mutation vs. 2 or more mutations). The p values are from Fisher's exact test.

Fig. 4. **Associations between the** *IL28B* **allele and HCV sequences.** The prevalence of HCV sequences predicting a resistant phenotype to IFN was higher in patients with the minor *IL28B* allele than those with major allele. (A) 0 or 1 mutation in the ISDR of NS5A, (B) Gln or His at Core70, and (C) Met at Core91. p values are from Fisher's exact test.

portion of patients with advanced fibrosis (F3-4) was 39% (84/217) in patients with low platelet counts (<140 × 10^9/L) compared to 13% (37/279) in those with high platelet counts (⩾140 × 10^9/L).

Validation of the data mining analysis

The results of the data mining analysis were validated with 165 patients who differed from those used for model building. Each patient was allocated to one of the six subgroups for the validation using the flow-chart form of the decision tree. The rate of SVR and NVR in each subgroup was calculated. The rates of SVR and NVR for each subgroup of patients were closely correlated between the model building and the validation patients (r^2 = 0.99 and 0.98) (Fig. 6).

Discussion

The rate of NVR after 48 weeks of PEG-IFN/RBV therapy among patients infected with HCV of genotype 1 is around 20–30%. Previously, there have been no reliable baseline predictors of NVR or SVR. Because more potent therapies, such as protease and polymerase inhibitor of HCV [28,29] and nitazoxianide [30], are in clinical trials and may become available in the near future, a pre-treatment prediction of the likelihood of response may be helpful for patients and physicians, to support clinical decisions about whether to begin the current standard of care or whether to wait for emerging therapies. This study revealed that the *IL28B* polymorphism was the overwhelming predictor of NVR and is independent of host factors and viral sequences reported previously. The *IL28B* encodes a protein also known as IFN-lambda 3, which is thought to suppress the replication of various viruses including HCV [31,32]. The results of the current study and the findings of the GWAS studies [6–9] may provide the rationale for developing diagnostic testing or an IFN-lambda based therapy for chronic hepatitis C in the future.

12%). After stratification by the *IL28B* allele, patients with low platelet counts (<140 × 10^9/L) had a lower probability of SVR and higher probability of NVR than those with high platelet counts (⩾140 × 10^9/L): for the minor *IL28B* allele, SVR was 7% vs. 19%, and NVR was 84% vs. 62%, and for the major *IL28B* allele, SVR was 32% vs. 66% and NVR was 16% vs. 8%. Among patients with the major *IL28B* allele and low platelet counts, those with two or more mutations in the ISDR had a higher probability of SVR and lower probability of relapse than those with one or no mutations in the ISDR (SVR: 75% vs. 27%, and relapse: 8% vs. 57%). Among patients with the major *IL28B* allele and high platelet counts, those with a low HCV-RNA titer (<600,000 IU/ml) had a higher probability of SVR and lower probability of NVR and relapse than those with a high HCV-RNA titer (SVR: 90% vs. 61%, NVR: 0% vs. 10%, and relapse: 10% vs. 29%). The sensitivity and specificity of the decision tree were 78% and 70%, respectively. The area under the receiver operating characteristic (ROC) curve of the model was 0.782 (data not shown). The pro-
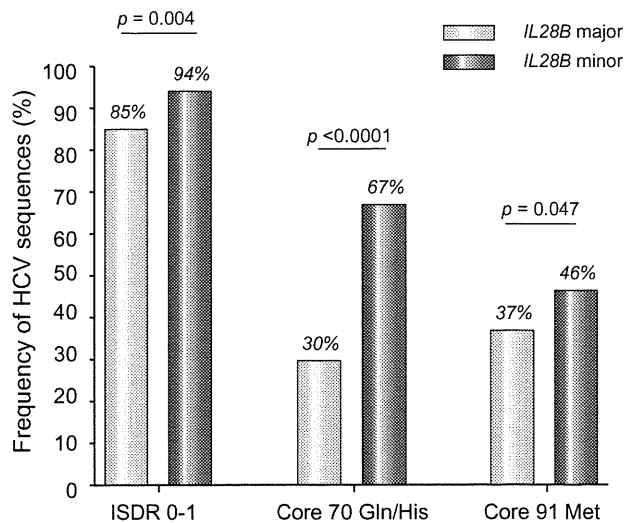
Table 2. Factors associated with NVR analyzed by univariate and multivariate logistic regression analysis.

	Univariate			Multivariate		
	Odds ratio	95%CI	p value	Odds ratio	95%CI	p value
Gender: female	0.98	0.67-1.45	0.938	1.29	0.75-2.23	0.363
Age	1.01	0.97-1.01	0.223	0.99	0.97-1.02	0.679
ALT	1.00	1.00-1.00	0.867	1.00	0.99-1.00	0.580
GGT	1.004	1.00-1.01	0.029	1.00	1.00-1.00	0.715
Platelets	0.95	0.91-0.99	0.009	0.92	0.87-0.98	0.006
Fibrosis: F3-4	2.23	1.46-3.42	0.0002	1.97	1.09-3.57	0.025
HCV-RNA: ≥600,000 IU/ml	1.83	1.05-3.19	0.035	2.49	1.17-5.29	0.018
ISDR mutation: ≤1	2.14	1.08-4.22	0.030	0.96	0.78-1.18	0.707
Core 70 (Gln/His)	3.23	2.16-4.78	<0.0001	1.41	0.83-2.42	0.207
Core 91 (Met)	1.39	0.95-2.06	0.093	1.21	0.72-2.04	0.462
IL28B: Minor allele	19.24	11.87-31.18	<0.0001	20.83	11.63-37.04	<0.0001

ALT, alanine aminotransferase; GGT, gamma-glutamyltransferase; ISDR, interferon sensitivity determining region; Gln, glutamine; His, histidine; Met, methionine; Minor allele, heterozygote or homozygote of minor allele.

Table 3. Factors associated with SVR analyzed by univariate and multivariate logistic regression analysis.

	Univariate			Multivariate		
	Odds ratio	95%CI	p value	Odds ratio	95%CI	p value
Gender: female	0.81	0.56-1.16	0.253	0.86	0.55-1.35	0.508
Age	0.97	0.95-0.99	0.0003	0.99	0.96-1.01	0.199
ALT	1.00	1.00-1.00	0.337	1.00	1.00-1.01	0.108
GGT	1.00	1.00-1.00	0.273	1.00	1.00-1.00	0.797
Platelets	1.12	1.01-116	<0.0001	1.13	1.08-1.19	<0.0001
Fibrosis: F0-2	2.64	1.65-4.22	<0.0001	1.87	1.07-3.28	0.029
HCV-RNA: <600,000 IU/ml	2.49	1.55-3.98	0.0001	2.75	1.55-4.90	0.001
ISDR mutation: 2≤	3.78	2.14-6.68	<0.0001	2.11	1.06-4.18	0.033
Core 70 (Arg)	1.61	1.11-2.28	0.012	0.84	0.52-1.35	0.470
Core 91 (Leu)	1.28	0.88-1.85	0.185	1.26	0.81-1.96	0.300
IL28B: Major allele	6.21	3.75-10.31	<0.0001	7.41	4.05-13.57	<0.0001

ALT, alanine aminotransferase; GGT, Gamma-glutamyltransferase; ISDR, interferon sensitivity determining region; Arg, arginine; Leu, leucine; Major allele, homozygote of major allele.

Among baseline factors, IL28B was the most significant predictor of NVR and SVR. Moreover, the IL28B allele type was also correlated with early virological response: the rate of RVR and cEVR was significantly high for the IL28B major allele compared to the IL28B minor allele: 9% vs. 3% for RVR and 57% vs. 11% for cEVR (Fig. 2). On the other hand, the relapse rate was not different between the IL28B genotypes within patients who achieved RVR or cEVR (Fig. 3). We believe that optimal therapy should be based on baseline features and a response-guided approach. Our findings suggest that the IL28B genotype is a useful baseline predictor of virological response which should be used for selecting the treatment regimen: whether to treat patients with PEG-IFN and RBV or to wait for more effective future therapy including direct acting antiviral drugs. On the other hand, baseline IL28B genotype might not be suitable for determining the treatment duration in patients who started PEG-IFN/RBV therapy and whose virological response is determined because the IL28B genotype is not useful for the prediction of relapse. The duration of therapy should be personalized based on the virological response. Future studies need to explore whether the combination of baseline IL28B genotype and response-guided approach further improves the optimization of treatment duration.

The SVR rate in patients having the IL28B minor allele was 14% in the present study while it was 23% in Caucasians and 9% in African Americans in a study by McCarthy et al. [33]. On the other hand, the SVR rate in patients having the IL28B minor allele was 28% in genotypes 1/4 compared to 80% in genotypes 2/3 in a study by Rauch et al. [9]. These data imply that the impact of the IL28B polymorphism on response to therapy may be different in terms of race, geographical areas, or HCV genotypes, and that our data need to be validated in future studies including different populations and geographical areas before generalization.

Table 4. Factors associated with IL28B genotype.

	IL28B major allele n = 345	IL28B minor allele n = 151	p value
Gender: male	166 (48%)	84 (56%)	0.143
Age (years)	57 ± 10	57 ± 10	0.585
ALT (IU/L)	79 ± 60	78 ± 62	0.842
Platelets (10⁹/L)	153 ± 54	155 ± 52	0.761
GGT (IU/L)	51 ± 45	78 ± 91	0.001
Fibrosis: F3-4	76 (22%)	45 (30%)	0.063
Steatosis:			
>10%	16/88 (18%)	13/23 (57%)	0.024
>30%	6/88 (7%)	6/23 (26%)	0.017
HCV-RNA: >600,000 IU/ml	284 (82%)	125 (83%)	1.000

ALT, alanine aminotransferase; GGT, gamma-glutamyltransferase.

Four GWAS studies have shown the association between a genetic polymorphism near the IL28B gene and response to PEG-IFN plus RBV therapy. The SNPs that showed significant association with response were rs12979860 [8] and rs8099917 [6,7,9]. There is a strong linkage-disequilibrium (LD) between these two SNPs as well as several other SNPs near the IL28B gene in Japanese patients [34] but the degree of LD was weaker in Caucasians and Hispanics [8]. Thus, the combination of SNPs is not useful for predicting response in Japanese patients but may improve the predictive value in patients other than Japanese who have weaker LD between SNPs.

Other significant predictors of response independent of IL28B genotype were platelet counts, stage of fibrosis, and HCV RVA load. A previous study reported that platelet count is a predictor of response to therapy [35], and the lower platelet count was related with advanced liver fibrosis in the present study. The association between response to therapy and advanced fibrosis independent of the IL28B polymorphism is consistent with a recent study by Rauch et al. [9].

There is agreement that the viral genotype is significantly associated with the treatment outcome. Moreover, viral factors such as substitutions in the ISDR of the NS5A region [10] or in the amino acid sequence of the HCV core [4] have been studied in relation to the response to IFN treatment. The amino acid Gln or His at Core70 and Met at Core91 are repeatedly reported to be associated with resistance to therapy [4,14,15] in Japanese patients but these data wait to be validated in different populations or other geographical areas. In this study, we confirmed that patients with two or more mutations in the ISDR had a higher rate of undetectable HCV-RNA at each time point during therapy. In addition, the rate of relapse among patients who achieved cEVR was significantly lower in patients with two or more mutations in ISDR compared to those with only one or no mutations (15% vs. 31%, p <0.05). Thus, the ISDR sequence may be used to predict a relapse among patients who achieved virological response during therapy, while the IL28B polymorphism may be used to predict the virological response before therapy. A higher number of mutations in the ISDR are reported to have close association with SVR in Japanese [11–13,15,36] or Asian [37,38] populations but data from Western countries have been controversial [39–42]. A meta-analysis of 1230 patients including 525 patients from Europe has shown that there was a positive correlation

between the SVR and the number of mutations in the ISDR in Japanese as well as in European patients [43] but this correlation was more pronounced in Japanese patients. Thus, geographical factors may account for the different impact of ISDR on treatment response, which may be a potential limitation of our study.

To our surprise, these HCV sequences were associated with the IL28B genotype: HCV sequences with an IFN resistant phenotype were more prevalent in patients with the minor IL28B allele than those with the major allele. This was an unexpected finding, as we initially thought that host genetics and viral sequences were completely independent. A recent study reported that the IL28B polymorphism (rs12979860) was significantly associated with HCV genotype: the IL28B minor allele was more frequent in HCV genotype 1-infected patients compared to patients infected with HCV genotype 2 or 3 [33]. Again, patients with the IL28B minor allele (IFN resistant genotype) were infected with HCV sequences that are linked to an IFN resistant phenotype. The mechanism for this association is unclear, but may be related to an interaction between the IL28B genotype and HCV sequences in the development of chronic HCV infection as discussed by McCarthy et al., since the IL28B polymorphism was associated with the natural clearance of HCV [44]. Alternatively, the HCV sequence within the patient may be selected during the course of chronic infection [45,46]. These hypotheses should be explored through prospective studies of spontaneous HCV clearance or by testing the time-dependent changes in the HCV sequence during the course of chronic infection.

How these host and viral factors can be integrated to predict the response to therapy in future clinical practice is an important question. Because various host and viral factors interact in the same patient, predictive analysis should consider these factors in combination. Using the data mining analysis, we constructed a simple decision tree model for the pre-treatment prediction of SVR and NVR to PEG-IFN/RBV therapy. The classification of patients based on the genetic polymorphism of IL28B, mutation in the ISDR, serum levels of HCV-RNA, and platelet counts, identified subgroups of patients who have the lowest probabilities of NVR (0%) with the highest probabilities of SVR (90%) as well as those who have the highest probabilities of NVR (84%) with the lowest probability of SVR (7%). The reproducibility of the model was confirmed by the independent validation based on a second group of patients. Using this model, we can rapidly develop an
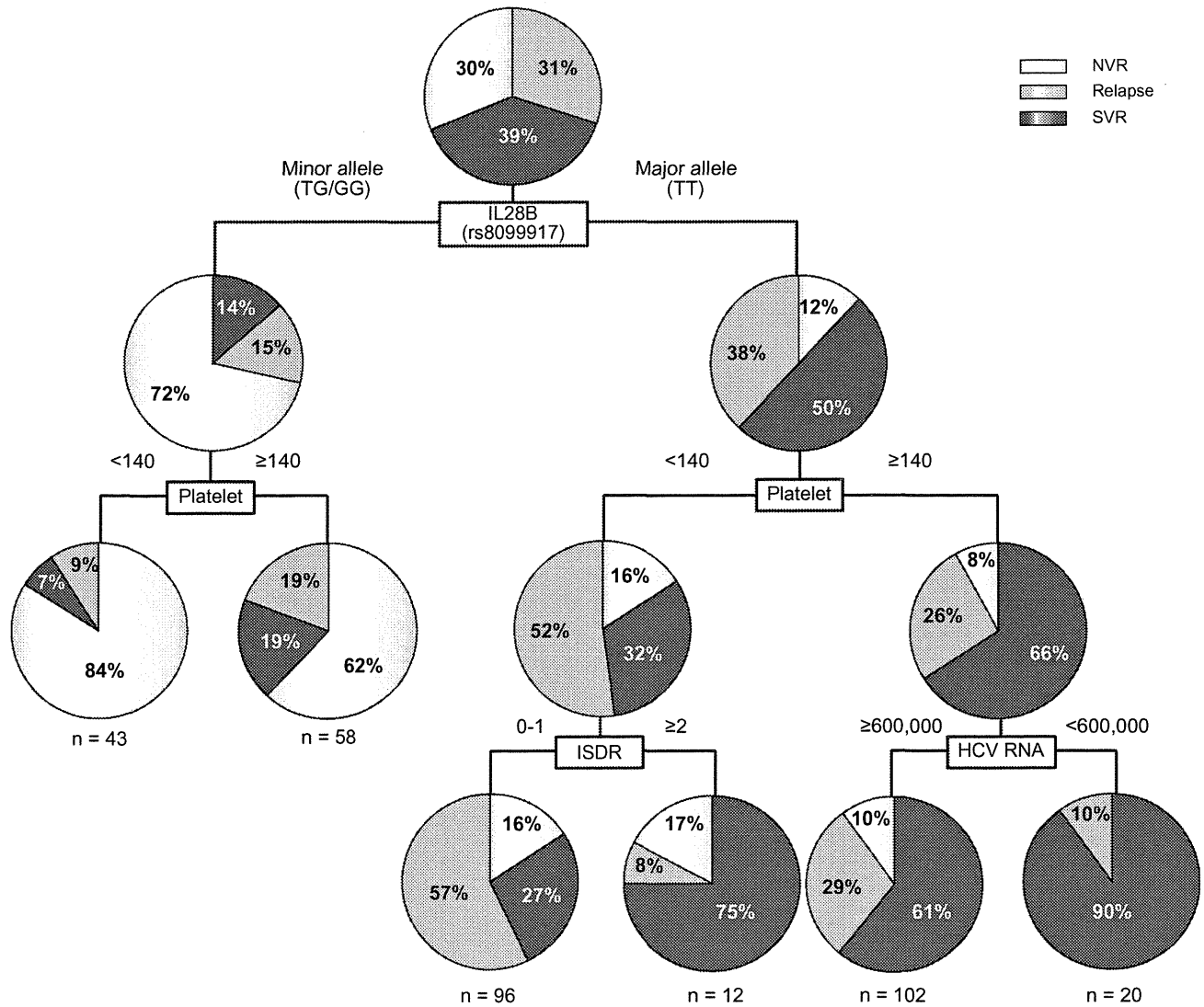
100
125

Fig. 5. Decision tree for the prediction of response to therapy. The boxes indicate the factors used for splitting. Pie charts indicate the rate of response for each group of patients after splitting. The rate of null virological response, relapse, and sustained virological response is shown.

estimate of the response before treatment, by simply allocating patients to subgroups by following the flow-chart form, which may facilitate clinical decision making. This is in contrast to the calculating formula, which was constructed by the traditional logistic regression model. This was not widely used in clinical practice as it is abstruse and inconvenient. These results support the evidence based approach of selecting the optimum treatment strategy for individual patients, such as treating patients with a low probability of NVR with current PEG-IFN/RBV combination therapy or advising those with a high probability of NVR to wait for more effective future therapies. Patients with a high probability of relapse may be treated for a longer duration to avoid a relapse. Decisions may be based on the possibility of a response against a potential risk of adverse events and the cost of the therapy, or disease progression while waiting for future therapy.

We have previously reported the predictive model of early virological response to PEG-IFN and RBV in chronic hepatitis C

[26]. The top factor selected as significant was the grade of steatosis, followed by serum level of LDL cholesterol, age, GGT, and blood sugar. The mechanism of association between these factors and treatment response was not clear at that time. To our interest, a recent study by Li et al. [47] has shown that high serum level of LDL cholesterol was linked to the *IL28B* major allele (CC in rs12979860). High serum level of LDL cholesterol was associated with SVR but it was no longer significant when analyzed together with the *IL28B* genotype in multivariate analysis. Thus, the association between treatment response and LDL cholesterol levels may reflect the underlining link of LDL cholesterol levels to *IL28B* genotype. Steatosis is reported to be correlated with low lipid levels [48] which suggest that *IL28B* genotypes may be also associated with steatosis. In fact, there were significant correlations between the *IL28B* genotype and the presence of steatosis in the present study (Table 4). In addition, the serum level of GGT, another predictive factor in our previous study, was signif-
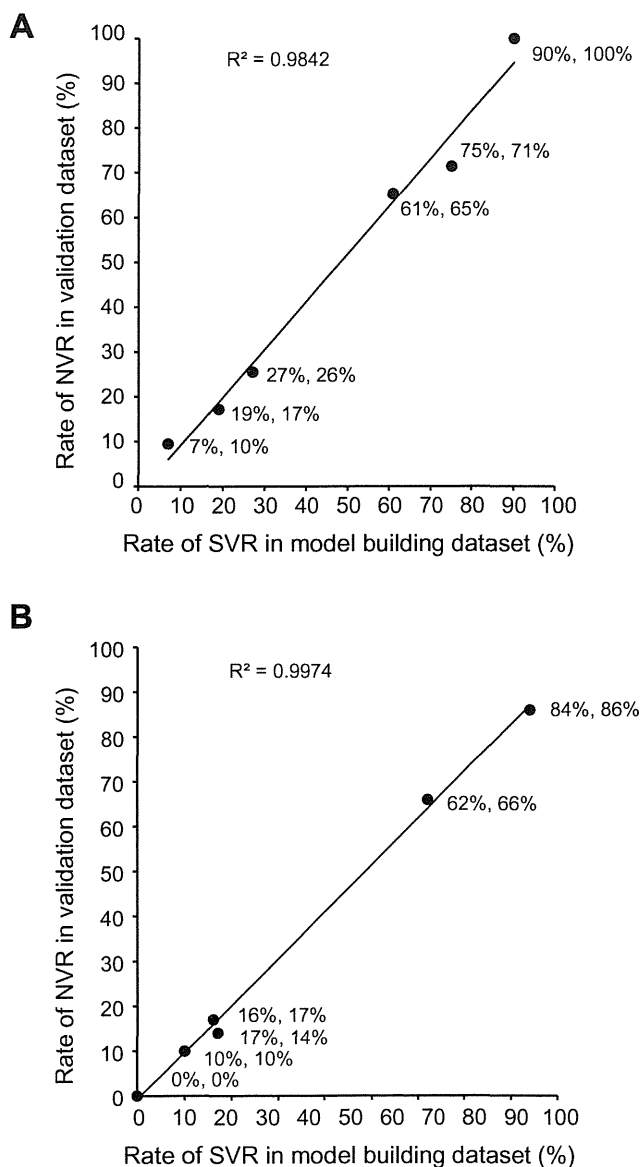
Fig. 6. **Validation of the CART analysis.** Each patient in the validation group was allocated to one of the six subgroups by following the flow-chart form of the decision tree. The rate of (A) sustained virological response (SVR) and (B) null virological response (NVR) in each subgroup was calculated and plotted. The X-axis represents the rate of SVR or NVR in the model building patients and the Y-axis represents those in the validation patients. The rate of SVR and NVR in each subgroup of patients is closely correlated between the model building and the validation patients (correlation coefficient: r^2 = 0.98–0.99).

icantly associated with *IL28B* genotype in the present study (Table 4). The serum level of GGT was significantly associated with NVR when examined independently but was no longer significant when analyzed together with the *IL28B* genotype. These observations indicate that some of the factors that we have previously identified may be associated with virological response to therapy through the underlining link to the *IL28B* genotype.

In conclusion, the present study highlighted the impact of the *IL28B* polymorphism and mutation in the ISDR on the pre-treatment prediction of response to PEG-IFN/RBV therapy. A decision model including these host and viral factors has the potential to

support selection of the optimum treatment strategy for individual patients, which may enable personalized treatment.

Conflict of interest

The authors who have taken part in this study declare that they do not have anything to disclose regarding funding or conflict of interest with respect to this manuscript.

References

[1] Ray Kim W. Global epidemiology and burden of hepatitis C. Microbes Infect 2002;4 (12):1219–1225.
[2] Fried MW, Shiffman ML, Reddy KR, Smith C, Marinos G, Goncales Jr FL, et al. Peginterferon alfa-2a plus ribavirin for chronic hepatitis C virus infection. N Engl J Med 2002;347 (13):975–982.
[3] Manns MP, McHutchison JG, Gordon SC, Rustgi VK, Shiffman M, Reindollar R, et al. Peginterferon alfa-2b plus ribavirin compared with interferon alfa-2b plus ribavirin for initial treatment of chronic hepatitis C: a randomised trial. Lancet 2001;358 (9286):958–965.
[4] Akuta N, Suzuki F, Sezaki H, Suzuki Y, Hosaka T, Someya T, et al. Association of amino acid substitution pattern in core protein of hepatitis C virus genotype 1b high viral load and non-virological response to interferon-ribavirin combination therapy. Intervirology 2005;48 (6):372–380.
[5] Davis GL, Wong JB, McHutchison JG, Manns MP, Harvey J, Albrecht J. Early virologic response to treatment with peginterferon alfa-2b plus ribavirin in patients with chronic hepatitis C. Hepatology 2003;38 (3):645–652.
[6] Tanaka Y, Nishida N, Sugiyama M, Kurosaki M, Matsuura K, Sakamoto N, et al. Genome-wide association of IL28B with response to pegylated interferon-alpha and ribavirin therapy for chronic hepatitis C. Nat Genet 2009;10:1105–1109.
[7] Suppiah V, Moldovan M, Ahlenstiel G, Berg T, Weltman M, Abate ML, et al. IL28B is associated with response to chronic hepatitis C interferon-alpha and ribavirin therapy. Nat Genet 2009;10:1100–1104.
[8] Ge D, Fellay J, Thompson AJ, Simon JS, Shianna KV, Urban TJ, et al. Genetic variation in IL28B predicts hepatitis C treatment-induced viral clearance. Nature 2009;461 (7262):399–401.
[9] Rauch A, Kutalik Z, Descombes P, Cai T, Di Iulio J, Mueller T, et al. Genetic variation in IL28B is associated with chronic hepatitis C and treatment failure: a genome-wide association study. Gastroenterology 2010;138 (4):1338–1345.
[10] Enomoto N, Sakuma I, Asahina Y, Kurosaki M, Murakami T, Yamamoto C, et al. Comparison of full-length sequences of interferon-sensitive and resistant hepatitis C virus 1b. Sensitivity to interferon is conferred by amino acid substitutions in the NS5A region. J Clin Invest 1995;96 (1):224–230.
[11] Enomoto N, Sakuma I, Asahina Y, Kurosaki M, Murakami T, Yamamoto C, et al. Mutations in the nonstructural protein 5A gene and response to interferon in patients with chronic hepatitis C virus 1b infection. N Engl J Med 1996;334 (2):77–81.
[12] Kurosaki M, Enomoto N, Murakami T, Sakuma I, Asahina Y, Yamamoto C, et al. Analysis of genotypes and amino acid residues 2209 to 2248 of the NS5A region of hepatitis C virus in relation to the response to interferon-beta therapy. Hepatology 1997;25 (3):750–753.
[13] Shirakawa H, Matsumoto A, Joshita S, Komatsu M, Tanaka N, Umemura T, et al. Pretreatment prediction of virological response to peginterferon plus ribavirin therapy in chronic hepatitis C patients using viral and host factors. Hepatology 2008;48 (6):1753–1760.
[14] Akuta N, Suzuki F, Kawamura Y, Yatsuji H, Sezaki H, Suzuki Y, et al. Predictive factors of early and sustained responses to peginterferon plus ribavirin combination therapy in Japanese patients infected with hepatitis C virus genotype 1b: amino acid substitutions in the core region and low-density lipoprotein cholesterol levels. J Hepatol 2007;46 (3):403–410.

[15] Okanoue T, Itoh Y, Hashimoto H, Yasui K, Minami M, Takehara T, et al. Predictive values of amino acid sequences of the core and NS5A regions in antiviral therapy for hepatitis C: a Japanese multi-center study. J Gastroenterol 2009;44 (9):952–963.

[16] Segal MR, Bloch DA. A comparison of estimated proportional hazards models and regression trees. Stat Med 1989;8 (5):539–550.

[17] LeBlanc M, Crowley J. A review of tree-based prognostic models. Cancer Treat Res 1995;75:113–124.

[18] Garzotto M, Beer TM, Hudson RG, Peters L, Hsieh YC, Barrera E, et al. Improved detection of prostate cancer using classification and regression tree analysis. J Clin Oncol 2005;23 (19):4322–4329.

[19] Averbook BJ, Fu P, Rao JS, Mansour EG. A long-term analysis of 1018 patients with melanoma by classic Cox regression and tree-structured survival analysis at a major referral center: implications on the future of cancer staging. Surgery 2002;132 (4):589–602.

[20] Leiter U, Buettner PG, Eigentler TK, Garbe C. Prognostic factors of thin cutaneous melanoma: an analysis of the central malignant melanoma registry of the german dermatological society. J Clin Oncol 2004;22 (18):3660–3667.

[21] Valera VA, Walter BA, Yokoyama N, Koyama Y, Iiai T, Okamoto H, et al. Prognostic groups in colorectal carcinoma patients based on tumor cell proliferation and classification and regression tree (CART) survival analysis. Ann Surg Oncol 2007;14 (1):34–40.

[22] Zlobec I, Steele R, Nigam N, Compton CC. A predictive model of rectal tumor response to preoperative radiotherapy using classification and regression tree methods. Clin Cancer Res 2005;11 (15):5440–5443.

[23] Thabane M, Simunovic M, Akhtar-Danesh N, Marshall JK. Development and validation of a risk score for post-infectious irritable bowel syndrome. Am J Gastroenterol 2009;104 (9):2267–2274.

[24] Wu BU, Johannes RS, Sun X, Tabak Y, Conwell DL, Banks PA. The early prediction of mortality in acute pancreatitis: a large population-based study. Gut 2008;57 (12):1698–1703.

[25] Fonarow GC, Adams Jr KF, Abraham WT, Yancy CW, Boscardin WJ. Risk stratification for in-hospital mortality in acutely decompensated heart failure: classification and regression tree analysis. Jama 2005;293 (5):572–580.

[26] Kurosaki M, Matsunaga K, Hirayama I, Tanaka T, Sato M, Yasui Y, et al. A predictive model of response to peginterferon ribavirin in chronic hepatitis C using classification and regression tree analysis. Hepatol Res 2010;40 (3):251–260.

[27] Nishida N, Tanabe T, Takasu M, Suyama A, Tokunaga K. Further development of multiplex single nucleotide polymorphism typing method, the DigiTag2 assay. Anal Biochem 2007;364 (1):78–85.

[28] Hezode C, Forestier N, Dusheiko G, Ferenci P, Pol S, Goeser T, et al. Telaprevir and peginterferon with or without ribavirin for chronic HCV infection. N Engl J Med 2009;360 (18):1839–1850.

[29] McHutchison JG, Everson GT, Gordon SC, Jacobson IM, Sulkowski M, Kauffman R, et al. Telaprevir with peginterferon and ribavirin for chronic HCV genotype 1 infection. N Engl J Med 2009;360 (18):1827–1838.

[30] Rossignol JF, Elfert A, El-Gohary Y, Keeffe EB. Improved virologic response in chronic hepatitis C genotype 4 treated with nitazoxanide, peginterferon, and ribavirin. Gastroenterology 2009;136 (3):856–862.

[31] Marcello T, Grakoui A, Barba-Spaeth G, Machlin ES, Kotenko SV, MacDonald MR, et al. Interferons alpha and lambda inhibit hepatitis C virus replication with distinct signal transduction and gene regulation kinetics. Gastroenterology 2006;131 (6):1887–1898.

[32] Robek MD, Boyd BS, Chisari FV. Lambda interferon inhibits hepatitis B and C virus replication. J Virol 2005;79 (6):3851–3854.

[33] McCarthy JJ, Li JH, Thompson A, Suchindran S, Lao XQ, Patel K, et al. Replicated association between an IL28B Gene Variant and a Sustained

Response to Pegylated Interferon and Ribavirin. Gastroenterology 2010;138:2307–2314.

[34] Tanaka Y, Nishida N, Sugiyama M, Tokunaga K, Mizokami M. Λ-interferons and the single nucleotide polymorphisms: a milestone to tailor-made therapy for chronic hepatitis C. Hepatol Res 2010;40:449–460.

[35] Backus LI, Boothroyd DB, Phillips BR, Mole LA. Predictors of response of US veterans to treatment for the hepatitis C virus. Hepatology 2007;46 (1):37–47.

[36] Mori N, Imamura M, Kawakami Y, Saneto H, Kawaoka T, Takaki S, et al. Randomized trial of high-dose interferon-alpha-2b combined with ribavirin in patients with chronic hepatitis C: correlation between amino acid substitutions in the core/NS5A region and virological response to interferon therapy. J Med Virol 2009;81 (4):640–649.

[37] Hung CH, Lee CM, Lu SN, Lee JF, Wang JH, Tung HD, et al. Mutations in the NS5A and E2-PePHD region of hepatitis C virus type 1b and correlation with the response to combination therapy with interferon and ribavirin. J Viral Hepat 2003;10 (2):87–94.

[38] Yen YH, Hung CH, Hu TH, Chen CH, Wu CM, Wang JH, et al. Mutations in the interferon sensitivity-determining region (nonstructural 5A amino acid 2209–2248) in patients with hepatitis C-1b infection and correlating response to combined therapy of pegylated interferon and ribavirin. Aliment Pharmacol Ther 2008;27 (1):72–79.

[39] Zeuzem S, Lee JH, Roth WK. Mutations in the nonstructural 5A gene of European hepatitis C virus isolates and response to interferon alfa. Hepatology 1997;25 (3):740–744.

[40] Squadrito G, Leone F, Sartori M, Nalpas B, Berthelot P, Raimondo G, et al. Mutations in the nonstructural 5A region of hepatitis C virus and response of chronic hepatitis C to interferon alfa. Gastroenterology 1997;113 (2):567–572.

[41] Sarrazin C, Berg T, Lee JH, Teuber G, Dietrich CF, Roth WK, et al. Improved correlation between multiple mutations within the NS5A region and virological response in European patients chronically infected with hepatitis C virus type 1b undergoing combination therapy. J Hepatol 1999;30 (6):1004–1013.

[42] Murphy MD, Rosen HR, Marousek GI, Chou S. Analysis of sequence configurations of the ISDR, PKR-binding domain, and V3 region as predictors of response to induction interferon-alpha and ribavirin therapy in chronic hepatitis C infection. Dig Dis Sci 2002;47 (6):1195–1205.

[43] Pascu M, Martus P, Hohne M, Wiedenmann B, Hopf U, Schreier E, et al. Sustained virological response in hepatitis C virus type 1b infected patients is predicted by the number of mutations within the NS5A-ISDR: a meta-analysis focused on geographical differences. Gut 2004;53 (9):1345–1351.

[44] Thomas DL, Thio CL, Martin MP, Qi Y, Ge D, O'Huigin C, et al. Genetic variation in IL28B and spontaneous clearance of hepatitis C virus. Nature 2009;461 (7265):798–801.

[45] Kurosaki M, Enomoto N, Marumo F, Sato C. Evolution and selection of hepatitis C virus variants in patients with chronic hepatitis C. Virology 1994;205 (1):161–169.

[46] Enomoto N, Kurosaki M, Tanaka Y, Marumo F, Sato C. Fluctuation of hepatitis C virus quasispecies in persistent infection and interferon treatment revealed by single-strand conformation polymorphism analysis. J Gen Virol 1994;75 (Pt 6):1361–1369.

[47] Li JH, Lao XQ, Tillmann HL, Rowell J, Patel K, Thompson A, et al. Interferon-lambda genotype and low serum low-density lipoprotein cholesterol levels in patients with chronic hepatitis C infection. Hepatology 1904;51 (6):1904–1911.

[48] Serfaty L, Andreani T, Giral P, Carbonell N, Chazouilleres O, Poupon R. Hepatitis C virus induced hypobetalipoproteinemia: a possible mechanism for steatosis in chronic hepatitis C. J Hepatol 2001;34 (3):428–434.

103
128

Clearance of hepatitis C in chimpanzees is associated with intrahepatic T-cell perforin expression during the late acute phase

H. Watanabe*, F. Wells and M. E. Major *Laboratory of Hepatitis Viruses, Division of Viral Products, Center for Biologics Evaluation and Research, Food and Drug Administration, Bethesda, MD, USA*

SUMMARY. The liver is the primary site of hepatitis C virus (HCV) replication. Therefore, we undertook detailed intrahepatic studies of T-cell dynamics, apoptosis, and gene expression during the acute phase of infection using liver biopsies from chimpanzees that developed persistent infection or spontaneously cleared the virus. We examined more than 40 liver biopsies histologically and quantitatively for T-cell infiltration, hepatocyte apoptosis and perforin expression. These data were correlated with outcome and viral kinetics. We observed intrahepatic T-cell infiltration in both groups of animals with CD8$^+$ T cells representing the major population. The appearance of T cells was always associated with apoptosis and mild alanine aminotransferase (ALT) elevations. Apoptosis (5–20% of hepatocytes) always occurred prior to serum ALT peak. Quantification of intrahepatic ALT mRNA revealed no upregulation of gene expression confirming that serum ALT increases were due to release of this enzyme from cells. During the late acute phase, cleared animals showed an increased frequency of hepatocyte apoptosis relative to persistently infected animals ($P < 0.05$). This correlated with a higher intrahepatic CD8$^+$ T-cell frequency in the cleared group ($P < 0.01$) with a greater proportion of lymphocytes expressing perforin compared with the persistent group ($P < 0.001$). All infected animals mounted intrahepatic immune responses during the acute phase, but these were not maintained in frequency or efficacy in persistent infections. There is a reduction in the numbers of intrahepatic T cells during the late acute phase in infections that become persistent with significantly fewer of these cells functional in clearing the virus by killing infected hepatocytes.

Keywords: hepatitis C virus, immune responses, intrahepatic, perforin, T cells, viral clearance.

INTRODUCTION

Infection with hepatitis C virus (HCV) poses serious public health problems. It frequently leads to chronic hepatitis and cirrhosis and is associated with hepatocellular carcinoma. Infection with this virus is considered to be one of the major risk factors for primary liver cancer [1]. Persistent infection occurs in up to 85% of patients [2] and between 30 and 60% of chimpanzees [3], although the mechanisms that lead up to this outcome are still undefined. The chimpanzee is the only animal model available to study pathogenesis of

this viral disease and represents well the features of HCV infection in humans, such as the kinetics of viraemia and persistent infection, even in the presence of immune responses [4,5].

It is assumed that HCV is controlled by a combination of innate and adaptive immune responses. One possible contributing mechanism is the destruction of infected hepatocytes by specific T cells through death receptors or the perforin/granzyme B pathway [6,7]. We previously showed through detailed studies of viral kinetics in acute phase chimpanzee infections that an early (within 1–2 weeks) type-I interferon (IFN) response contributes to a slowing of viral replication, but does not lead to reductions in titres [8,9]. However, a rapid decline in peripheral HCV RNA levels coincides precisely with increased IFN-γ expression in the livers of chimpanzees and the appearance of CD8$^+$ T-cell responses [8–10].

The analysis of intrahepatic apoptosis during HCV infection has been mainly confined to the chronic phase, where it is thought to contribute to long-term liver damage [11,12]. There has been little opportunity to study apoptosis during

the acute phase in humans because of the lack of tissue samples, problems identifying acute infections and clinical complications associated with liver biopsies. It is still unknown whether the process of hepatocyte apoptosis is linked to clearance or persistence of HCV and to what extent hepatocyte death is associated with intrahepatic T-cell infiltration or function. It has been suggested that apoptosis induction upon HCV infection may contribute to liver pathology, but that inhibition of apoptosis, through viral mechanisms, may result in persistence of the virus. Chimpanzee studies are invaluable for analysing acute phase intrahepatic responses and more specifically the association between hepatocyte destruction and viral clearance.

Using quantitative methods, we have studied the dynamics of hepatocyte death, intrahepatic T cells, cellular signals and gene expression in sequential liver biopsies from chimpanzees acutely infected with a monotypic virus (1a genotype). We have been able to address the role of liver apoptosis in acute phase infection, specifically to determine if there is a difference in hepatic apoptosis during infections that clear and those that go on to persist.

MATERIALS AND METHODS

Challenge inoculum

The chimpanzees in this study were challenged intrahepatically with in vitro transcribed RNA [13] or intravenously with monoclonal HCV [14]. The infection profiles and acute phase viral kinetics have been previously reported [8]. Table 1 shows challenge inocula together with time and values of peak ALT and RNA titres. Liver biopsies were obtained biweekly, portions were formalin-fixed and paraffin-embedded or snap-frozen in liquid nitrogen. Negative controls for all tests were represented by samples from each individual animal taken prior to challenge.

Chimpanzees

The housing, maintenance and care of the chimpanzees used in this study met requirements for the humane use of animals in scientific research as defined by the National Institutes of Health.

Relative quantification of ALT mRNA

Reverse transcription (RT) of RNA from liver biopsies was carried out as previously described [14]. Relative mRNA levels were determined using primer/probe sets for human ALT and the endogenous control Glyceraldehyde 3-phosphate dehydrogenase, obtained from Applied Biosystems (Foster City, CA, USA) and used according to the manufacturer's instructions. Relative mRNA quantification was calculated using the comparative C_T method [14].

Histological staining

Formalin-fixed paraffin-embedded liver sections (5 μm) were stained with haematoxylin–eosin for histological assessment. Unstained sections were treated for antigen retrieval by boiling in citrate buffer (5 × 5 s in a microwave followed by cooling for 10 min). Sections were blocked with 10% normal goat serum (2 h) and incubated overnight with primary antibodies at 4°C. For the laser scanning cytometer (LSC) analysis (see below), anti-CD4$^+$ (clone 4B12) and anti-CD8$^+$ (clone C8/144B) antibodies were used (Dako, Carpinteria, CA, USA) with Alexa Fluor 647 anti-mouse IgG. Sections were counterstained with 4′,6-diamidine-2-phenylindole. Perforin and the cleaved cytokeratin-18 (CK18) were assessed using the LSAB–HRP staining kit (Dako) and anti-perforin or M30 (anti-CK18 cleavage product) monoclonal antibodies as previously described [15]. Reaction product was developed with 3,3′-diaminobenzidine and light counterstaining was obtained with haematoxylin. Data were expressed as the percentage of liver infiltrating lymphocytes or hepatocytes positive for perforin or cleaved CK18, respectively.

Apoptosis analysis: TUNEL staining

DNA fragmentation was visualized using the in situ cell death detection kit (TMR Red or fluorescein isothiocyanate (FITC); Roche, Indianapolis, IN, USA). Sections labelled in the absence of terminal deoxynucleotidyl transferase were used as negative controls and sections pretreated with DNase I were used as positive controls. Sections were scanned using the LSC (see below) and the level of TUNEL staining expressed as a percentage of the whole surface of the tissue section.

ID	Sex	Inoculum dosage	ALT peak Value (IU/mL)	ALT peak Time (weeks)	RNA peak Titre/mL (Log10)	RNA peak Time (weeks)	Outcome
1535	M	RNA*	360	17	6.42	14	Persistent
6412	F	100 CID$_{50}$	642	9	7.48	7	Persistent
1605	F	3.2 CID$_{50}$	176	9	6.04	7	Cleared
1606	F	RNA*	297	9	5.36	8	Cleared

Table 1 Challenge inocula, time and values of peak ALT and RNA titres for chimpanzees included in this study

*In vitro transcribed RNA was delivered intrahepatically.

Caspase activation in serum

Serum samples diluted at 1:100 were tested for the CK18 cleavage product using the M30-Apoptosense ELISA kit (PEVIVA, DiaPharma, West Chester, OH, USA) according to the manufacturer's instructions.

Laser scanning cytometer analysis

Tissue sections (5 μm) were analysed on an LSC2 (Compu-cyte, Cambridge, MA, USA) [16]. The LSC is equipped with Argon, Helium/Neon (HeNe) and UV lasers and in a similar manner to flow cytometry, the machine measures fluores-cent signal from labelled tissue or cells immobilized on a glass slide [17]. FITC and APC-annexin were detected through a 530/30-nm FITC filter and through a 650 long pass filter, respectively. Data were acquired and analysed with Wincyte acquisition software version 3.7 (Compucyte). Measurements of FITC and APC-annexin were made on a log scale. Data were acquired using phantom contouring that covered the entire tissue section.

Statistical analyses

The Student's *t*-test was used for comparison of the propor-tion of cells staining positive for specific markers in the two groups of animals.

RESULTS

Apoptosis in acute phase HCV-infected liver

TUNEL staining in sequential biopsies over a 24-week period for two chimpanzees that developed persistent infections (Ch1535 and Ch6412) and for two animals that cleared HCV (Ch1605 and Ch1606) is shown in Fig. 1. For reference, the viral RNA titres and ALT elevations over the same time period

for each animal are shown in the upper panels. As is typically seem for acute phase infections, viral RNA titres increased exponentially in the first 2–3 weeks followed by a slower increase in titres during the following 4–6 weeks [8,9]. Titres began to decline coincident with ALT elevations and either reached a plateau (in the persistently infected animals) or decreased below detectable levels and the virus was eventually cleared. The proportion of the liver section positive for TUNEL staining was determined through scanning using the LSC with background, negative and positive region gates, assigned using positive and negative control tissue sections. An example of the histogram data obtained from liver biopsy sections from Ch1535 is shown in Fig. S1.

Prechallenge liver biopsies from all animals (week 0) exhibited minimal (<1%) TUNEL staining, but in both groups apoptosis occurred early after HCV infection, reach-ing levels between 2 and 7% by week 4 (Fig. 1, lower pan-els). The maximum apoptosis observed on whole liver biopsy sections using TUNEL staining was 16%. There was appar-ently no correlation between peak levels of TUNEL staining and ALT peaks. There was a trend towards higher levels of TUNEL staining during the early to middle acute phase in animals that developed persistent infections than in animals clearing infection while the reverse was true for the late acute phase (post week 20).

Although TUNEL staining is widely used for the detection of apoptosis and can provide useful data, there exist limita-tions in sensitivity and specificity [18], mainly because of the fact that this technique only detects fragmentation of the nucleus which is a late phase event in the apoptotic process. Therefore, we employed a second, histological staining method to specifically study hepatocyte apoptosis through staining with the mAb M30. This recognizes a neo-epitope exposed when CK18 is cleaved by caspase during the early stages of apoptotic DNA fragmentation [19]. Figure 2 shows the level of this early phase caspase activity in hepatocytes. Overall, we observed higher levels of positive hepatocytes in
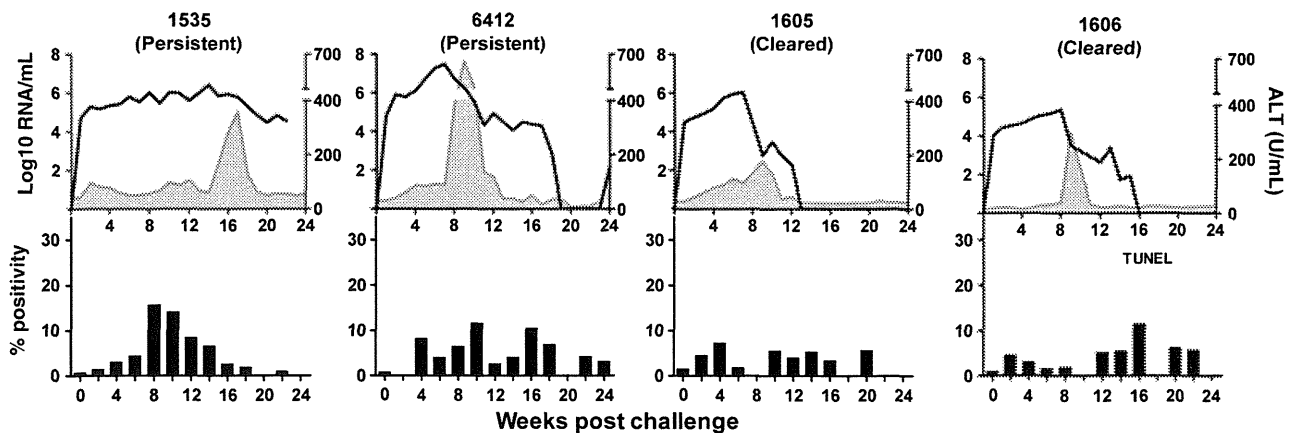

Fig. 1 Apoptosis in liver biopsies from acute phase infections of chimpanzees as assessed by TUNEL assay. TUNEL staining is shown on the lower panels together with ALT elevations (greyed area under the curve) and viral RNA titres (solid black lines) on the upper panels. (a) Ch1535; (b) Ch6412; (c) Ch1605; (d) Ch1606.
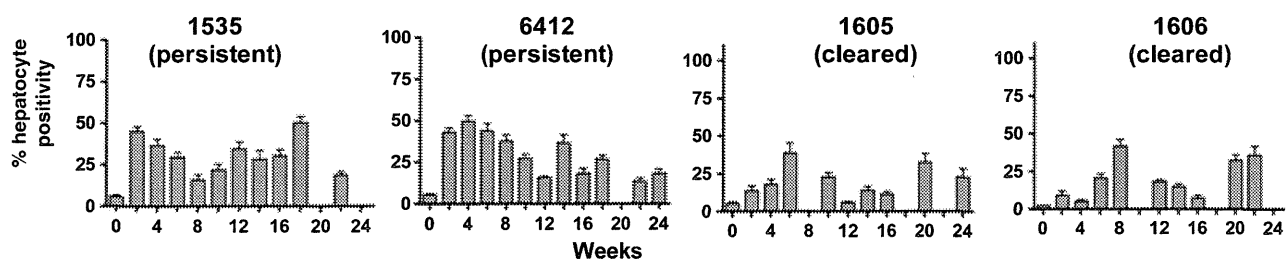
Fig. 2 Apoptosis in hepatocytes of biopsies from acute phase infections of chimpanzees as assessed by staining using the monoclonal antibody M30 that recognizes the neo-epitope of CK18 exposed following caspase cleavage, calculated by dividing the number of CK18 positive hepatocytes by the total number of hepatocytes counted within a field of view (5–12 fields of view were counted depending upon the size of the tissue section). Error bars represent SE of the mean.

tissue sections using M30 antibody, up to 50% during the early acute phase. The frequency of positive cells was higher using this technique than when using TUNEL staining, because of the greater sensitivity of M30 antibody staining, the specific analysis of hepatocytes and the fact that using the TUNEL technique, the entire liver section, including nonparenchymal tissue, was stained and assessed for apoptosis. However, the pattern of apoptosis was similar using both methods in that CK18 cleavage is observed early after infection, within 2–4 weeks, and peak levels did not coincide with ALT peaks. The CK18 cleavage signal was higher for the animals that developed persistent infections during the early to middle acute phase, but lower for these animals during the late acute phase (Fig. 2).

The levels of CK18 cleavage product in weekly serum samples were also assessed using an ELISA that selectively recognizes the proteolytic neo-epitope of CK18. Using this method, the levels of serum caspase activity have been shown to correlate with ALT elevations and liver pathology in chronically infected patients [15]. In our study, no substantial elevations of antigen in chimpanzee sera were observed at any point during the first 26 weeks of infection (data not shown).

ALT elevations are not associated with increased ALT mRNA expression

In order to confirm the source of serum ALT elevations, we analysed the ALT mRNA level in sequential liver biopsies from two animals that developed persistent infections and from three animals that cleared HCV. We found that ALT mRNA levels remained at or below baseline throughout the acute phase infection in the majority of samples regardless of disease outcome and increases in ALT mRNA (reaching a maximum of sixfold above baseline) did not coincide with serum ALT elevations (data not shown).

Intrahepatic T-cell infiltration during acute phase infections

Sequential liver biopsies were examined for T-cell infiltration through immunohistological staining using anti-CD4$^+$ and

anti-CD8$^+$ antibodies. The proportion of liver biopsy positive for these T-cell markers was assessed using the LSC and phantom contours. We observed increases in intrahepatic T-cell infiltration (5- to 10-fold above baseline) in both groups of animals, with CD8$^+$ cells representing the major population throughout infection (Fig. 3). In two animals [1535 (persistent) and 1605 (cleared)], the onset of T-cell infiltration was as early as 2 weeks postinfection, but in all animals the appearance of T cells in the liver was associated with liver apoptosis and mild ALT elevations (compare Figs 1–3). Consistent with the data obtained for liver apoptosis, cleared animals showed an increased frequency of intrahepatic T-cell infiltration (8- to 10-fold above baseline) in the late acute phase. This increase was not observed in the animals that developed persistent infections.

Liver sections from these same time points were examined for perforin expression through immunohistochemistry. Stained sections were visualized by light microscopy and infiltrating lymphocytes positive for perforin staining were scored. Data were expressed as the percentage of perforin-positive cells within 5–12 fields of view (Fig. 4). At time zero, few or no cells were found to be perforin positive, but following infection the proportions increased in all animals with no distinctive pattern during the first 10–12 weeks associated with outcome. However, at later time points, weeks 18–24, up to 20% of the infiltrating lymphocytes in liver sections from the cleared animals stained positive for perforin, whereas only 1–2% of the intrahepatic cells in the persistently infected group were positive for this marker. This frequency of perforin expression is independent of the number of liver infiltrating lymphocytes, as we performed direct immunohistochemical staining and expressed the value as a proportion of total cells counted.

Statistical analyses of CK18 cleavage, T-cell counts and perforin expression

We made statistical comparisons using the Student's *t*-test for the two groups of animals: hepatocytes staining positive for the CK18 cleavage product and cells staining positive for CD4$^+$ and CD8$^+$ or perforin. To perform this analysis, we divided the first 24 weeks of acute infection into three phases, early
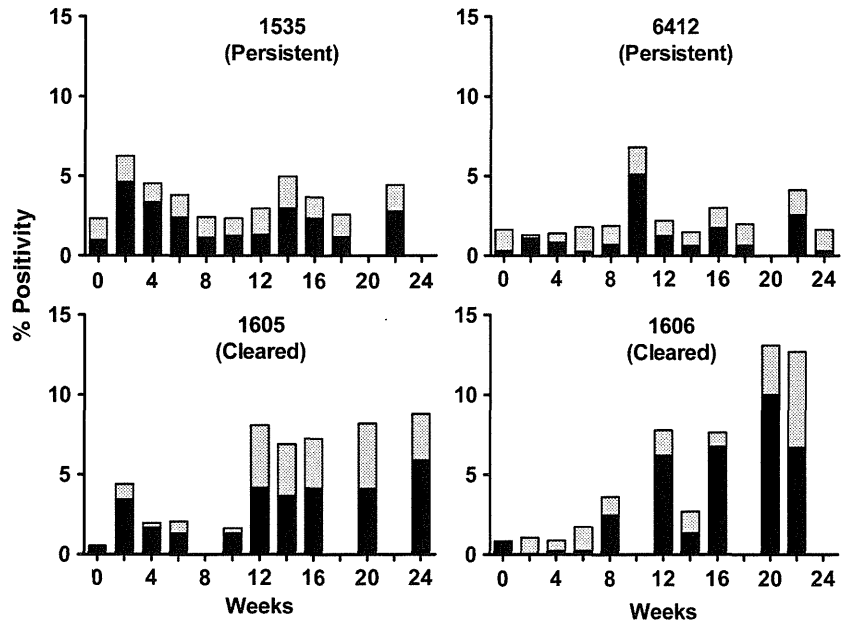
Fig. 3 T-cell infiltration in liver biopsies from acute phase infections of chimpanzees. CD4$^+$ (grey bars) and CD8$^+$ (black bars) T-cell frequency is shown as assessed by LSC analysis of liver biopsy sections.
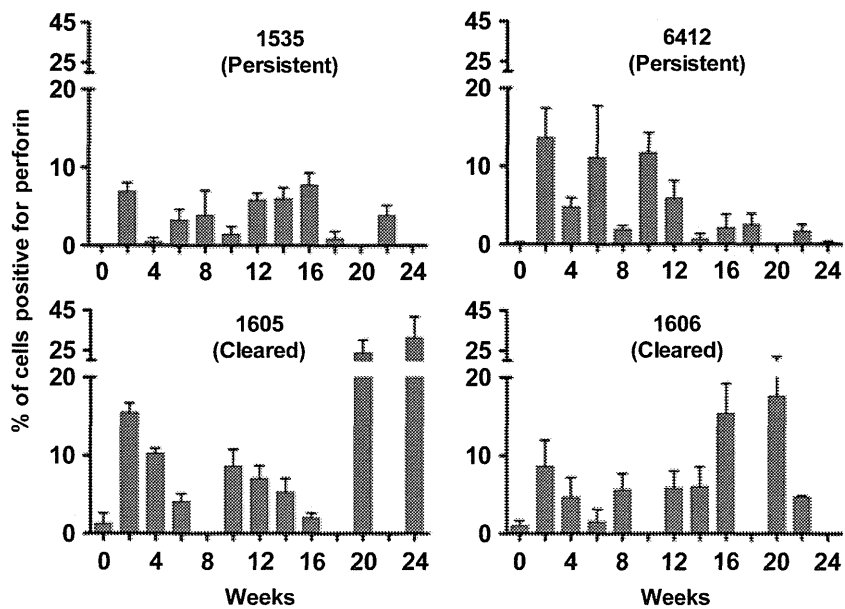

Fig. 4 Perforin expression in liver infiltrating cells during acute phase infection. Percentage of positivity is expressed as the percentage of cells positive for perforin staining in chimpanzee liver biopsies calculated by dividing the number of perforin positive cells by the total number of liver infiltrating cells counted within a field of view (5–12 fields of view were counted depending upon the size of the tissue section). Error bars represent SE of the mean.

(weeks 0–8), middle (weeks 10–16) and late (weeks 18–24). We found statistically significant differences for each of the parameters of CK18 cleavage, intrahepatic CD4$^+$ and CD8$^+$ T-cell infiltration and perforin expression at different time points postinfection (Fig. 5). Moderate variations in the defined weeks for these time periods were applied such that the middle and late acute phases were represented by weeks 10–16 and 18–24, respectively. The parameters at each phase showed similar statistical differences.

CK18 cleavage

As shown above, hepatocytes from both groups of animals displayed signs of apoptosis from early stages postinfection.

When the proportion of hepatocytes positive for CK18 cleavage was compared between the groups (Fig. 5a), we found a statistically higher level of positive hepatocytes in the animals that developed persistent infections in the early $(P = 0.0003)$ and middle $(P < 0.0001)$ acute phases, whereas this pattern was reversed at the late acute phase with a higher proportion of hepatocytes entering apoptosis in the livers of the animals that cleared the virus $(P = 0.0174)$.

CD4$^+$ and CD8$^+$ frequency

CD4$^+$ and CD8$^+$ cells were detected in all animals beginning very early postinfection (Fig. 3). Statistical comparison showed no significant difference during the first 8 weeks of
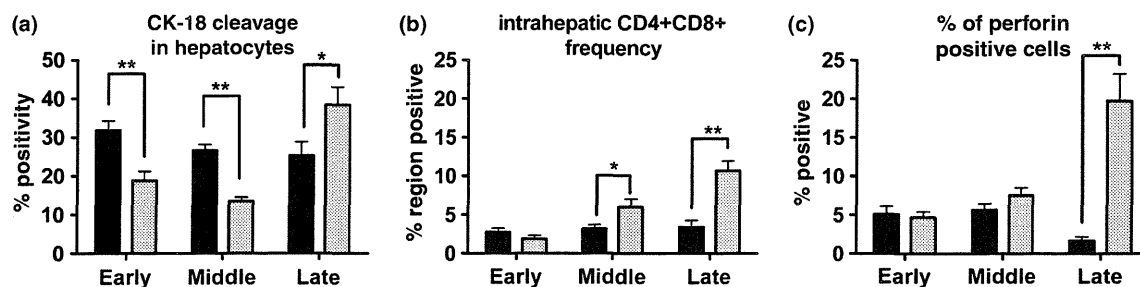
Fig. 5 Statistical comparisons of apoptosis, T-cell infiltration and perforin staining in liver biopsies during acute phase infection. Early, middle and late acute phases are defined as weeks 1–8 (early), 10–16 (middle) and 18–24 (late). *$P < 0.05$; **$P < 0.01$. Each bar represents the mean value of data collected for the two animals in each group. Black bars represent data from animals that developed persistent infections; grey bars represent data from animals that cleared virus. Error bars represent SE of the mean.

infection (Fig. 5b) ($P = 0.217$), but animals that cleared the virus had higher numbers of intrahepatic CD4$^+$ and CD8$^+$ T cells during the middle ($P = 0.0424$) and late ($P = 0.0006$) phases.

Perforin expression in liver infiltrating lymphocytes

During the early and middle phases of infection, the perforin expression in cells was not statistically different between the two groups (Fig. 5c; $P = 0.82$ and $P = 0.14$ for the early and middle phases, respectively), suggesting that although there was a slightly higher level of intrahepatic T-cell infiltration in the cleared group, cells were equally functional regardless of the disease outcome. The greatest difference for perforin expression was seen at the late acute phase where there were ~10 times as many cells expressing perforin in the animals that cleared HCV than in those that did not ($P < 0.0001$).

DISCUSSION

Intrahepatic events that occur during acute phase HCV infections are difficult to analyse in detail. Most intrahepatic studies have been performed in chronically infected patients and the majority of such studies use biopsy specimens taken from one sample date. The chimpanzee studies described here not only provide an opportunity to analyse intrahepatic events during acute phase infection, but the use of sequential biopsies provides a measure of consistency between samples enabling us to correlate these events with viral kinetics and disease outcome.

Previous analyses of apoptosis in human liver samples from chronically infected patients have shown an association between apoptosis and liver injury [20,21]. Using a novel ELISA that recognizes the cleaved CK18 product, caspase activity has also been detected in the sera of HCV patients with inflammatory and fibrotic liver damage despite normal aminotransferase levels [15], potentially providing a sensitive noninvasive method of detecting early liver injury. In our hands, this ELISA was not sensitive enough to detect caspase activity in the serum, as it has been shown to do in chronically infected patients [15]. The levels of cleaved CK18

in chronic patients were associated with inflammatory and fibrotic liver damage, suggesting more severe or prolonged cell death is required for changes in serum caspase levels to be detectable with this assay.

We found that apoptosis occurs soon after infection in the chimpanzee livers during acute phase infections and that this activity preceded ALT elevations in all cases (Figs 1 & 2). This early acute phase apoptosis is probably because of innate immune responses induced by the initial viral infection. The innate immune response can directly activate macrophages in the liver and natural killer (NK) cells that can then mediate killing of infected cells [12]. In addition, viral infections alone can induce type-I IFN that can lead to cell death through the caspase pathways [22]. We have previously shown that 2′5 oligoadenylate synthetase, an IFN-α-induced protein, is detectable within 2 weeks of HCV infection in chimpanzee liver [8]. This data is consistent with virus-induced apoptosis occurring in the liver during the early phase of HCV infection, which although leading to hepatocyte death and a slowing of HCV replication is insufficient to decrease the titres or eliminate the virus.

Mild ALT elevations are often observed in chimpanzee studies during the first few weeks of infection [8] and can be seen for Ch1535, Ch6412 and Ch1605 in this study (Fig. 1). However, it appears that the serum ALT peaks, at levels several fold above baseline, occur as a consequence of earlier events that cause stress on the liver. An absence of correlation between ALT elevations and liver injury or HCV titres has been previously reported in chronic patients [20,23,24]. There is also the underlying question of whether ALT elevations are due to liver stress and hepatocyte killing or to elevated expression of this gene in liver cells, possibly because of regeneration of the liver following cell destruction. Using real-time RT-PCR on liver biopsies, we were able to establish that there is no correlation between serum ALT elevations and changes in ALT mRNA levels. In all the animals studied, ALT mRNA levels remained close to baseline during the acute phase confirming that ALT elevations are indeed because of increased secretion of this enzyme by cells.

We clearly show in this study that hepatocyte apoptosis occurs during the acute phase in both groups of animals. There is a greater frequency of apoptosis during the early and middle phase of infection in animals where the virus becomes persistent ($P < 0.01$, Fig. 5). This higher level of apoptosis correlates with higher viral titres in the persistent group and although temporally the ALT peaks do not coincide with apoptosis, we have shown previously that persistent infections are associated with higher ALT elevations and higher peak virus titres during the acute phase [8]. Thus, during the early and middle acute phases, persistent infections are associated with greater levels of apoptosis. However, we hypothesize that this is more a consequence of higher viral replication which cannot be completely cleared, despite intrahepatic T-cell infiltration and hepatocyte killing, rather than apoptosis directly contributing to the development of persistence. This may be a simple case of the immune system being unable to keep pace with the viral replication and correlates with previous studies of intrahepatic T cells in acute phase chimpanzee infections [10].

In this study, we also show that CD4 and CD8 T-cell infiltration is an early event (Fig. 3) with a proportion of these T cells able to produce perforin (Fig. 4), suggesting functionally active T cells that lead to the killing of infected hepatocytes. The perforin/granzyme B pathway has been implicated as one of the major mechanisms for clearance of noncytolytic viruses [6,7]. Many studies have shown the importance of T cells in acute phase infection and in prevention of HCV persistence [10,25–27]. However, as we have hypothesized from our previous studies of viral kinetics in acute phase chimpanzee infections [8,9], innate and adaptive immune responses are induced even in infections that result in persistence and the clearance or persistence of virus does not hinge on the early induction of intrahepatic immune responses.

It is during the late acute phase (16–24 weeks postinfection) where the differences in intrahepatic T-cell infiltration and function are most striking. At this stage of the infection, we show that there are significantly fewer T cells in the liver of animals that develop persistent infections ($P < 0.01$) and of these a significantly smaller proportion are functional as assessed by perforin expression ($P < 0.001$) (Fig. 5). This suggests that although an immune response is induced in those animals that develop persistent infections, it is not a fully adaptive response with a possible absence of clonal expansion and differentiation of specific T cells into effector cells, such that a continued clearance of virus does not take place. It is also possible that the intrahepatic T cells induced during the acute phase undergo a high level of apoptosis as has been described for chronic HCV patients [28], leading to fewer effector T cells in the liver at the later acute phase time point. We did not detect a substantially higher level of apoptosis from late phase liver sections using TUNEL staining; however, this method which examines the whole tissue may not be sensitive enough to pick up individual T-cell apoptosis. Other cells, such as NK cells, can be stained with

anti-CD8 antibody and can produce perforin. We did not specifically double stain cells during CD8 and perforin staining in order to differentiate T cells; however, although NK cells my play a role early during infection as part of the innate immune response, the major intrahepatic cell types involved in the adaptive immune response that controls or clears HCV are assumed to be T cells.

The normal liver contains significantly higher proportions of activated, effector and memory cells as well as NK/NK T cells compared with other tissues [29]. The mechanism for the retention or recruitment of T cells in the liver from lymphoid tissue or the circulating blood has not been identified but preferential recruitment of T cells, based on phenotypic markers, as they recirculate through the liver may play a major role [30,31]. During infections, T cells are recruited to the liver through a multi-step process of cytokine and chemokine expression [32]. It is still unclear whether T-cell priming takes place exclusively in the draining lymph nodes or whether hepatocytes, Kupffer cells, liver sinusoidal epithelial cells or dendritic cells present in the liver can prime T cells. Our data indicate differences between the outcome of infection could be due to T-cell recruitment to the liver and function of these T cells during the middle and late acute phases. We previously showed an absence in proliferative capacity of peripheral blood mononuclear cells in a vaccinated chimpanzee that developed a persistent infection postchallenge [33] and an association between proliferative capacity and perforin expression in $CD8^+$ T cells of HIV nonprogressors has also been shown [34]. Our data suggest similar mechanisms of immune evasion and viral persistence may exist in HCV infections. Further analyses of the intrahepatic T-cell subsets or intrahepatic chemokine expression in our cohort of animals during acute phase infection may help to explain the loss of immune control that leads to persistence of the virus.

ACKNOWLEDGEMENTS

REFERENCES

1 Bosch FX, Ribes J, Diaz M, Cleries R. Primary liver cancer: worldwide incidence and trends. *Gastroenterology* 2004; 127: S5–S16.

2 Alter MJ, Margolis HS, Krawczynski K *et al.* The natural history of community-acquired hepatitis C in the United States. *New Engl J Med* 1992; 327: 1899–1905.

3 Bassett SE, Brasky KM, Lanford RE. Analysis of hepatitis C virus-inoculated chimpanzees reveals unexpected clinical profiles. *J Virol* 1998; 72: 2589–2599.

4 Walker CM. Comparative features of hepatitis C virus infection in humans and chimpanzees. *Springer Semin Immunopathol* 1997; 19: 85–98.

5 Grakoui A, Hanson HL, Rice CM. Bad time for Bonzo? Experimental models of hepatitis C virus infection, replication, and pathogenesis. *Hepatology* 2001; 33: 489–495.

6 Lowin B, Hahne M, Mattmann C, Tschopp J. Cytolytic T-cell cytotoxicity is mediated through perforin and Fas lytic pathways. *Nature* 1994; 370: 650–652.

7 Kagi D, Vignaux F, Ledermann B *et al.* Fas and perforin pathways as major mechanisms of T cell-mediated cytotoxicity. *Science* 1994; 265: 528–530.

8 Major ME, Dahari H, Mihalik K *et al.* Hepatitis C virus kinetics and host responses associated with disease and outcome of infection in chimpanzees. *Hepatology* 2004; 39: 1709–1720.

9 Dahari H, Major M, Zhang X *et al.* Mathematical modeling of primary hepatitis C infection: noncytolytic clearance and early blockage of virion production. *Gastroenterology* 2005; 128: 1056–1066.

10 Thimme R, Bukh J, Spangenberg HC *et al.* Viral and immunological determinants of hepatitis C virus clearance, persistence, and disease. *Proc Natl Acad Sci U S A* 2002; 99: 15661–15668.

11 Guicciardi ME, Gores GJ. Apoptosis: a mechanism of acute and chronic liver injury. *Gut* 2005; 54: 1024–1033.

12 Fischer R, Baumert T, Blum HE. Hepatitis C virus infection and apoptosis. *World J Gastroenterol* 2007; 13: 4865–4872.

13 Kolykhalov AA, Agapov EV, Blight KJ, Mihalik K, Feinstone SM, Rice CM. Transmission of hepatitis C by intrahepatic inoculation with transcribed RNA. *Science* 1997; 277: 570–574.

14 Major ME, Mihalik K, Puig M *et al.* Previously infected and recovered chimpanzees exhibit rapid responses that control hepatitis C virus replication upon rechallenge. *J Virol* 2002; 76: 6586–6595.

15 Bantel H, Lugering A, Heidemann J *et al.* Detection of apoptotic caspase activation in sera from patients with chronic HCV infection is associated with fibrotic liver injury. *Hepatology* 2004; 40: 1078–1087.

16 Kamentsky LA, Kamentsky LD, Fletcher JA, Kurose A, Sasaki K. Methods for automatic multiparameter analysis of fluorescence in situ hybridized specimens with a laser scanning cytometer. *Cytometry* 1997; 27: 117–125.

17 Darzynkiewicz Z, Bedner E, Li X, Gorczyca W, Melamed MR. Laser-scanning cytometry: a new instrumentation with many applications. *Exp Cell Res* 1999; 249: 1–12.

18 Labat-Moleur F, Guillermet C, Lorimier P *et al.* TUNEL apoptotic cell detection in tissue sections: critical evaluation and improvement. *J Histochem Cytochem* 1998; 46: 327–334.

19 Leers MP, Kolgen W, Bjorklund V *et al.* Immunocytochemical detection and mapping of a cytokeratin 18 neo-epitope exposed during early apoptosis. *J Pathol* 1999; 187: 567–572.

20 Bantel H, Lugering A, Poremba C *et al.* Caspase activation correlates with the degree of inflammatory liver injury in chronic hepatitis C virus infection. *Hepatology* 2001; 34: 758–767.

21 Bantel H, Schulze-Osthoff K. Apoptosis in hepatitis C virus infection. *Cell Death Differ* 2003; 10(Suppl. 1): S48–S58.

22 Balachandran S, Roberts PC, Kipperman T *et al.* Alpha/beta interferons potentiate virus-induced apoptosis through activation of the FADD/Caspase-8 death signaling pathway. *J Virol* 2000; 74: 1513–1523.

23 Calabrese F, Pontisso P, Pettenazzo E *et al.* Liver cell apoptosis in chronic hepatitis C correlates with histological but not biochemical activity or serum HCV-RNA levels. *Hepatology* 2000; 31: 1153–1159.

24 Kronenberger B, Ruster B, Lee JH *et al.* Hepatocellular proliferation in patients with chronic hepatitis C and persistently normal or abnormal aminotransferase levels. *J Hepatol* 2000; 33: 640–647.

25 Grakoui A, Shoukry NH, Woollard DJ *et al.* HCV persistence and immune evasion in the absence of memory T cell help. *Science* 2003; 302: 659–662.

26 Shoukry NH, Grakoui A, Houghton M *et al.* Memory CD8$^+$ T cells are required for protection from persistent hepatitis C virus infection. *J Exp Med* 2003; 197: 1645–1655.

27 Folgori A, Spada E, Pezzanera M *et al.* Early impairment of HCV-specific T-cell proliferation during acute infection leads to failure of viral clearance. *Gut* 2006; 55: 1012–1019.

28 Radziewicz H, Ibegbu CC, Hon H *et al.* Impaired hepatitis C virus (HCV)-specific effector CD8$^+$ T cells undergo massive apoptosis in the peripheral blood during acute HCV infection and in the liver during the chronic phase of infection. *J Virol* 2008; 82: 9808–9822.

29 Norris S, Collins C, Doherty DG *et al.* Resident human hepatic lymphocytes are phenotypically different from circulating lymphocytes. *J Hepatol* 1998; 28: 84–90.

30 Klugewitz K, Adams DH, Emoto M, Eulenburg K, Hamann A. The composition of intrahepatic lymphocytes: shaped by selective recruitment? *Trends Immunol* 2004; 25: 590–594.

31 Klugewitz K, Blumenthal-Barby F, Eulenburg K, Emoto M, Hamann A. The spectrum of lymphoid subsets preferentially recruited into the liver reflects that of resident populations. *Immunol Lett* 2004; 93: 159–162.

32 Crispe IN. Hepatic T cells and liver tolerance. *Nat Rev Immunol* 2003; 3: 51–62.

33 Puig M, Mihalik K, Tilton JC *et al.* CD4$^+$ immune escape and subsequent T-cell failure following chimpanzee immunization against hepatitis C virus. *Hepatology* 2006; 44: 736–745.

34 Migueles SA, Laborico AC, Shupert WL *et al.* HIV-specific CD8$^+$ T cell proliferation is coupled to perforin expression and is maintained in nonprogressors. *Nat Immunol* 2002; 3: 1061–1068.

SUPPORTING INFORMATION

Additional Supporting Information may be found in the online version of this article

Figure S1. Laser Scanning Cytometry (LSC) histogram data for sequential liver biopsies from Ch1535. Titles across the top of each histogram refer to the week number post infection with the % of positive contours shown in